KTH Technology and Health

Finite element analysis of the effects of head-supported mass on neck responses

Complete Phase Three Report

Peter Halldin, PhD
Sofia Hedenstierna MSc.
Karin Brolin, PhD
Prof. Hans von Holst, M.D, PhD.

September 2006

UNITED STATES ARMY
EUROPEAN RESEARCH OFFICE OF THE U.S. ARMY
London, England

Contract NO: N62558-03-C-0013

Royal Institute of Technology, School of Technology and Health, Division of Neuronic Engineering, Stockholm, Sweden.
(peterh@kth.se)

Report Documentation Page

Form Approved
OMB No. 0704-0188

1. REPORT DATE	2. REPORT TYPE	3. DATES COVERED
SEP 2006	**N/A**	**-**

4. TITLE AND SUBTITLE	5a. CONTRACT NUMBER
Finite Element Analysis of the Effects of Head-Supported Mass on Neck Responses	5b. GRANT NUMBER
	5c. PROGRAM ELEMENT NUMBER
6. AUTHOR(S)	5d. PROJECT NUMBER
	5e. TASK NUMBER
	5f. WORK UNIT NUMBER
7. PERFORMING ORGANIZATION NAME(S) AND ADDRESS(ES) **Royal Institute of Technology, School of Technology and Health, Division of Neuronic Engineering Stockholm, Sweden**	8. PERFORMING ORGANIZATION REPORT NUMBER
9. SPONSORING/MONITORING AGENCY NAME(S) AND ADDRESS(ES)	10. SPONSOR/MONITOR'S ACRONYM(S)
	11. SPONSOR/MONITOR'S REPORT NUMBER(S)

12. DISTRIBUTION/AVAILABILITY STATEMENT
Approved for public release, distribution unlimited

13. SUPPLEMENTARY NOTES
The original document contains color images.

14. ABSTRACT

15. SUBJECT TERMS

16. SECURITY CLASSIFICATION OF:			17. LIMITATION OF ABSTRACT	18. NUMBER OF PAGES	19a. NAME OF RESPONSIBLE PERSON
a. REPORT	b. ABSTRACT	c. THIS PAGE			
unclassified	**unclassified**	**unclassified**	**SAR**	**45**	

Finite element analysis of the effects of head-supported mass on neck responses

Peter Halldin, PhD

Sofia Hedenstierna MSc.

Karin Brolin, PhD

Prof. Hans von Holst, M.D, PhD.

Royal Institute of Technology

Div. of Neuronic Engineering

Contract NO: N62558-03-C-0013

Complete Phase Three Report

October 2005 – September 2006

The research reported in this document has been made possible through the support and sponsorship of the U.S. Government through its European Research Office of the U.S. Army This report is intended only for the internal management use of the Contractor and U.S. Government.

Abstract

Technical Objectives:

The objectives for the whole project were to:

I. determine the relationships between head supported mass and the risk of neck injuries. The results should be used in a Graphical user interface. In this phase three report has also the Graphical User Interphase (GUI) been evaluated and the question about the how the muscle activation affect the injury risk.

II. to develop and implement a 3D numerical muscle model.

Method: Ad. I was done using a detailed Finite Element (FE) model of the human neck developed at the Royal Institute of Technology, Stockholm, Sweden. Ad. II was based on an FE model with a new geometry of the cervical spine.

I. The simulation matrix included seven impact situations (frontal, rear end, lateral, vertical, and oblique impacts in the horizontal plane, frontal plane, and sagittal plane.), three impact severities (5, 13.5 and 22 G), three helmet masses (1, 2 and 3 kg), and nine locations of the Center of Gravity of the helmet (offset relative to the CG of the head with -2, 0, 2, 4 and 6 cm in the superior/inferior and anterior/posterior directions). The neck model with just enough muscle activation to keep the head and helmet in upright position was compared with the model set to 100% activation of the neck muscle force. The GUI was evaluated using helmet inertial properties from two real helmets in use by the US Army.

II. The Suboccipital muscles, Deep dorsal muscles, Ventral muscles, Muscles linking the skull with the shoulder girdle and the Muscles linking the vertebral column with the scapulas and the ribcage have been modeled using 4 node solid elements for the passive properties and spring elements for the active part. The surfaces defining the muscles in the cervical spine were detected by segmentation from MR-scans using the software AMIRA. The surfaces were then smoothed and adjusted using the software Hypermesh. The meshing of the muscles was then performed with the software Truegrid. Contacts were defined between the interacting muscles. The new muscle model has been compared to a model with a spring muscle model for both the passive and the active part.

Results:

I. The KTH neck model has successfully been used to generate results for the GUI. Results from all simulations have been reported and sent to Titan Corporation that is contracted by USAARL to program the GUI. The GUI that uses an interpolation method to calculate the neck injury risk for a general helmet with a user defined HSM configuration shows to give realistic interpolated values compared to the FE model of the neck.

II. The 3D muscle model for the cervical spine includes 22 pairs of muscles. The solid muscle model showed to stabilize the vertebral column better than the spring muscle model. The model is still under evaluation and need further validation to be used in the HSM evaluation project.

Keywords

Finite element analysis, cervical spine, injury, prevention, muscles

Content

1 Background

Today, helmet mounted devises (HMD) or head supported mass (HSM) increases the mass of the helmets worn by soldiers. Complaints of neck pain during and after flight have increased amongst helicopter pilots and it is not clearly understood how the HMD affects the risks for neck injuries. Many volunteer studies have investigated how different helmet configurations affect the response in the human neck. Epidemiological studies have investigated the injury risk for helmet users in the army and presented different injury risk curves where the helmet mass and CG shift of the helmet are the parameters. However, there are uncertainties in the risk curves and more research on this topic was therefore necessary. Therefore, the objective of this project is to determine the relationships between head supported mass and the risk for neck injuries. This has been done using a detailed finite element (FE) model of the human neck developed at the Royal Institute of Technology [Halldin et al. 2000, Halldin 2001, Brolin 2002, Brolin and Halldin 2003, Kleiven 2002, Brolin et al, 2005], called the KTH neck model.

This report covers the third year of a three year project. The three year project includes five tasks of which three have been partly covered in this year, Table 1. The five tasks are:

A: Study of the effects of head-supported mass
B: Literature survey on muscle modeling with focus on muscle activation
C: Anatomical correct representation of the muscles
D: Modeling of neurological tissue
E: Indirect and direct head impacts

Table 1: Time schedule as presented in the project proposal.

		Time (work effort in months)			
Project	**Description**	**Year 1**	**Year 2**	**Year 3**	**TOTAL**
A	Effects of HSM	9	6	4	19
B	Litterature Survey	3			3
C	Muscle modelling	10	12	5	27
D	Spinal cord modelling	3	6	6	15
E	Modelling of impacts to head			9	9
Total		25	24	24	73

1.1 Summary from phase 1 (Year 1)

The KTH neck model was validated for an oblique impact in the sagittal plane (oblique XZ) (Bass et al. 2004), rear end impact (Davidsson et al 2002), oblique impact in the frontal plane (oblique XY) (Ewing et al 1976), vertical impact (AFRL Biodynamics Data Bank 199405-VDT3292) and lateral impact (Ewing et al. 1976). After tuning the activation of the neck musculature the KTH neck model correlated well to all impact directions. Simulations were then performed for three different helmet masses (2, 3 and 4kg) and five different positions of the helmet center of gravity (CG) in both the X (anterior/posterior) and Z (superior/inferior) direction. The accelerations applied to the KTH neck model were taken from the respective experimental study. Figure 1 illustrates the results summarized in arrows for five load cases. The risk charts were based on tissue level injury criteria, such as failure strain for the individual ligament, disc pressure and disc fiber strain. The results showed that the injury risk increases with helmet masses for all impact directions. The recommendation for the best position of the CG differs from load case to load case. Moving the CG horizontally in the anterior direction will give increased risk for injury in the oblique XZ, rear end impact and the vertical impact. In oblique XY and lateral impact an anterior shift of the CG will reduce the risk for an injury. Moving the CG in the superior direction will increase the risk for injury in the rear impact, oblique XY impact and the

lateral impact, and consequently not for the oblique XZ and the vertical impact. It was concluded that it is possible to use a detailed FE model to generate risk charts used for recommendations in helmet design. However, it has been shown that it is important to know what impact scenarios the wearer of the helmet is most likely to be subjected to.

The result from the first year is summarized in Figure 1 and is presented in detail in the Complete Phase One Report (Halldin et al. 2004a).

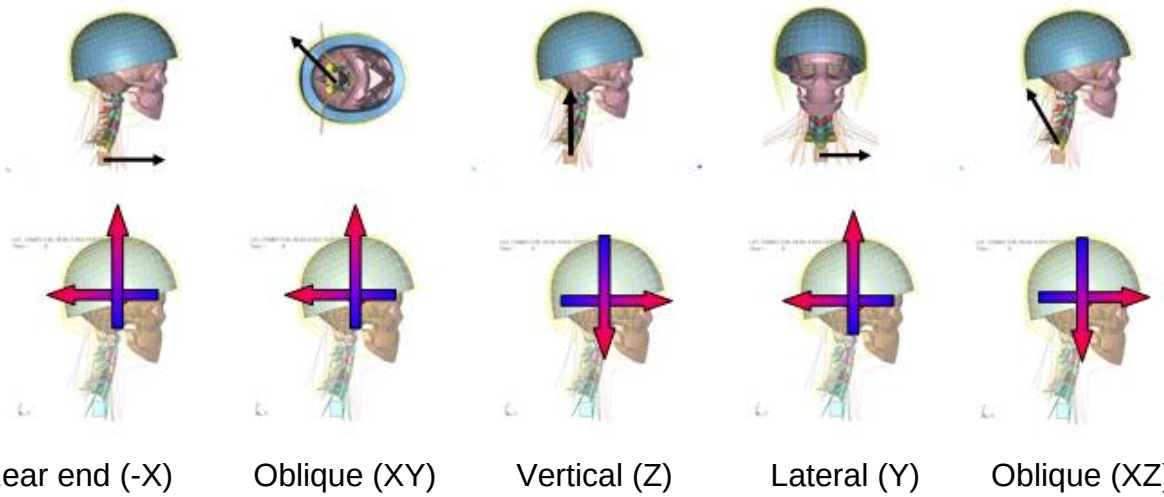

Figure 1. The top row shows the direction of the T1 acceleration load pulse. The bottom row shows the effect of CG shifts of the helmet mass. The arrows are pointing in the directions that result in increased injury risk when the CG is moved.

1.2 Summary from phase 2 (Year 2)

The main topics during year two were:

I. To compare the KTH neck model with cadaver component tests.

II. To determine the relationships between head supported mass and the risk of neck injuries. The results should be used in a Graphical user interface.

III. To develop and implement a 3D numerical muscle model.

Method: Ad. I and II were done using a detailed Finite Element (FE) model of the human neck developed at the Royal Institute of Technology, Stockholm, Sweden. Ad. III was based on an FE model with a new geometry of the cervical spine.

I. The KTH neck model was positioned up-side down as in the cadaver experiment performed by Bass et al (2004). The load was applied to the T2 vertebrae and results were computed for the linear and rotational accelerations, forces and moments at T1 and local stresses and strains in the bone, disc and ligaments.

II. The simulation matrix included seven impact situations (frontal, rear end, lateral, vertical, and oblique impacts in the horizontal plane, frontal plane, and sagittal plane.), three impact severities (5, 13.5 and 22 G), three helmet masses (1, 2 and 3 kg), and nine locations of the Center of Gravity of the helmet (offset relative to the CG of the head with -2, 0, 2, 4 and 6 cm in the superior/inferior and anterior/posterior directions).

III. Surfaces defining the important muscles in the cervical spine were detected by segmentation from MR-scans using the software AMIRA. The surfaces were then smoothed and adjusted using the software Hypermesh. The meshing of the muscles was then performed with the software Truegrid.

Results:

I. The KTH neck model kinematics and ligament tolerance levels compared well with what was found in the cadaver experiments by Bass et al. (2004).

II. Results from all simulations have been reported and sent to Titan Corporation that is contracted by USAARL to build a web based Graphical User Interface.

III. The surfaces for the 3D muscle model are positioned for a supine spine lordosis. To get the correct interaction between the muscles each muscle has to be positioned manually for an upright lordosis. This task and the subsequent meshing of the muscles have been delayed.

The results have been delivered to Titan Corporation in San Diego for implementation in the Graphical User Interface (GUI) in terms of all output files from the simulations. These output files are defined in Section 5 Deliverables. The following results are presented:

- BC values (according to Bass et al. 2004).
- Normalized ligament deformation.
- Normalized stresses in the compact and trabecular bone.

The results show that an increase of helmet mass increases all calculated values from the KTH neck model. Moving the centre of mass for the helmet in the positive X direction increases the risk of injury for the vertical, oblique XZ, and oblique YZ impacts, while it reduces the risk for injury in the rear end, oblique XY, lateral, and frontal impacts.

Moving the centre of mass in the positive Z-direction increases the risk for injury in the oblique XY, lateral, and frontal impacts, while it reduces the risk for injury in the rear end, vertical, oblique XZ and oblique YZ impacts. The results are summarized in Appendix A. These results correlate to the previous presented results in Halldin et al. 2004 (Figure 1).

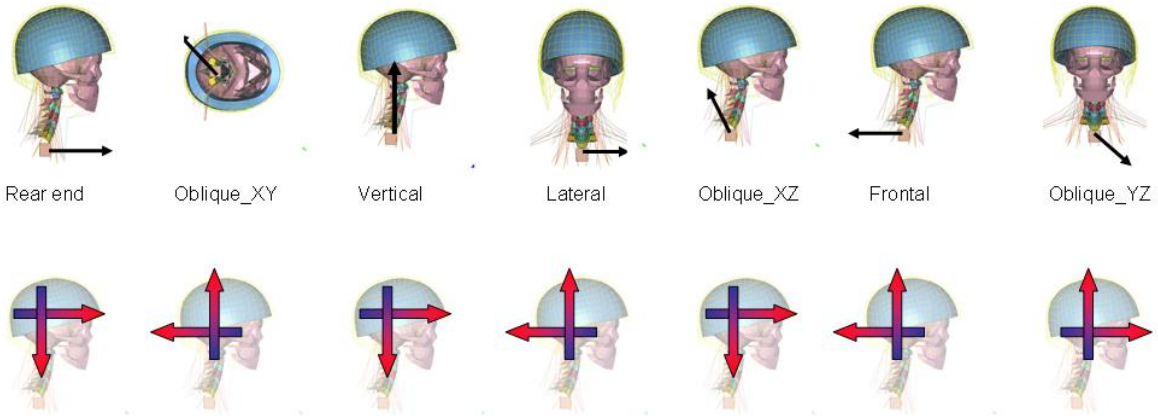

Figure 2. The top row shows the direction of the T1 acceleration load pulse. The bottom row shows the effect of CG shifts of the helmet mass. The arrows are pointing in the directions that result in increased injury risk when the CG is moved.

2 Introduction to the third year

This phase 3 final report covers months 25-36 of the total 36 months. The result from the first year and second year is presented in Halldin et al. 2004 and Halldin et al. 2005. The third year has been focused on tasks A and C. The project partners (KTH and USAARL) decided that the planned time in Task D and E should instead be on Task A and C.

The contractor has presented results from the project at three conferences during 2006. The first was a panel meeting at the ASMA annual conference 18th of May in Orlando. The second was in July at ICrash 2006 Conference in Greece and the third was at the World Congress of Biomechanics 4th of August in Munich.

3 Task A, Study of the effects of head-supported mass

This Section presents the results during the third year of Task A. In this phase an existing FE model of the neck has been used, called the KTH neck model (Halldin et al. 2004 and Brolin et al. 2005).

Section 3.1, describes the simulations preformed to fill the simulation matrix of a Graphical User Interface (GUI).

3.1 Method

The KTH neck model is developed in the FE code LSDYNA, Hallquist (1998). The KTH neck model includes the head, the seven cervical vertebras C1 to C7, the two uppermost thoracic vertebras T1 and T2 represented by cubes, the intervertebral discs, the 12 largest muscle groups and all spinal ligaments, Halldin (2001), Brolin (2002) and Brolin et al. (2004). The KTH neck model was used to simulate helicopter maneuvers and other standard risk situations for soldiers. In order to compare the different impact directions it was decided to use identical boundary conditions like impact energies, helmet masses and CG positions for the different impact directions. The project coordinator decided that seven impact scenarios should be studied. The coordinate system of the KTH neck model and the performed simulations are defined in Figure 2 and 3.

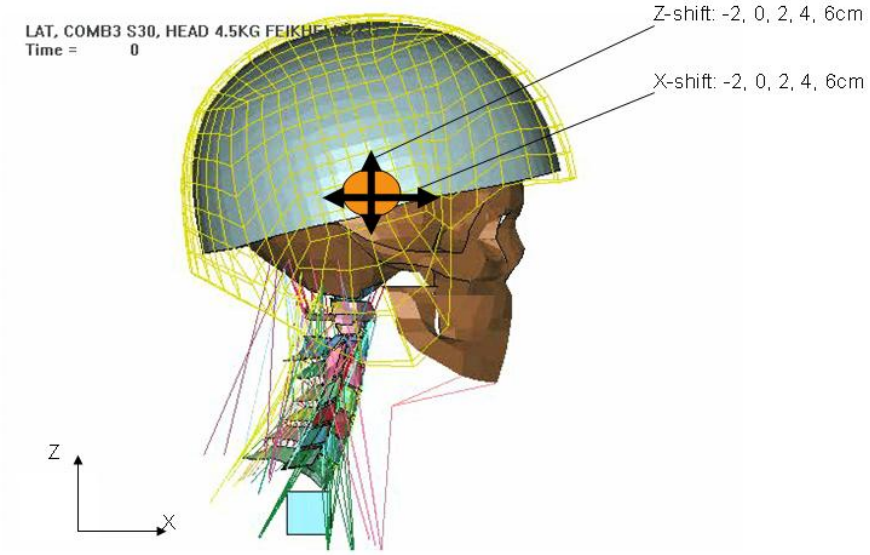

Figure 2. The KTH neck model.

3.1.1 Simulation plan for the GUI

In the project meeting on the 19th of April in San Diego and it was concluded that KTH should cover:

- Seven impact situations: pure frontal, rear end, lateral, and vertical impacts, and oblique impacts in the horizontal plane, frontal plane, and sagittal plane, according to Figure 3.The horizontal plane oblique impact was directed at an angle of 45 degrees to the sagittal plane and is called the oblique XY impact. The sagittal plane oblique impact was directed at an angle of 60 degrees to the horizontal plane and is called the oblique XZ impact. The frontal plane oblique impact is directed at an angle of 45 degrees to the horizontal plane and is called the oblique YZ impact.
- Three impact severities (5, 13.5 and 22G).
- Three helmet masses (1, 2 and 3kg)
- Five CG-offsets of the helmet, in the X-direction, relative to the CG of the head (-2, 0, 2, 4 and 6cm).
- Five CG-offsets of the helmet, in the Z-direction, relative to the CG of the head (-2, 0, 2, 4 and 6cm).
- Two different levels of muscle activation (*Relaxed* and *Tensed)*.

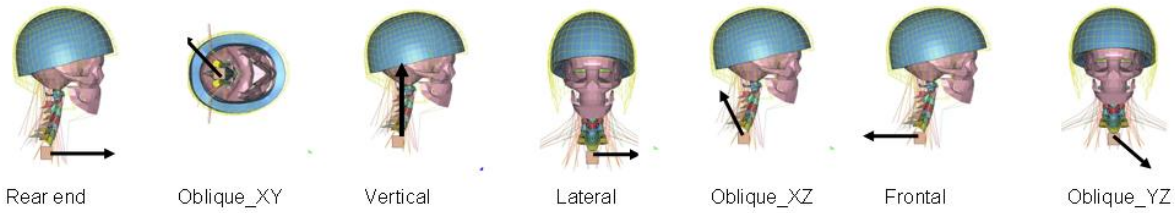

Figure 3. Figure showing the different impact directions. The black arrows show the direction of the T1 acceleration load pulse.

This gives a total of 7x3x3x5x5=1575 simulations. This large number of simulations would take about 1.5 month to run on an 8-node PC-cluster. In addition it would generate an enormous amount of data (approximately 1000 GB). Therefore, it was decided to use an interpolation method to minimize the number of simulations needed. The Box-Wilson Central Composite Faced (CCF) method, takes samples at the corners of the cube spanning up the simulation volume, and thereby allows the user to perform interpolations in these areas (NIST 2006). With the CCF method the number of simulations could be reduced from 225 simulations per impact direction to only 28 simulations, Table 2. This makes 196 simulations in total.

Table 2. The simulation matrix for one impact direction, the oblique XZ impact.

Baseline conditions

Simulation Number	Impact Direction	Impact level(G)	Helmet Weight (kg)	Weight COM X-direction (cm)	Weight COM Z-direction (cm)	Activation
1	XZ60	5	0	0	0	Relaxed
2	XZ60	5	0	0	0	Relaxed
3	XZ60	5	0	0	0	Relaxed

Central Composite Faced (CCF) Design

Simulation Number	Impact Direction	Impact level(G)	Helmet Weight (kg)	Weight COM X-direction (cm)	Weight COM Z-direction (cm)	Activation
4	XZ60	5	1	-2	-2	Relaxed
5	XZ60	5	1	-2	6	Relaxed
6	XZ60	5	1	6	-2	Relaxed
7	XZ60	5	1	6	6	Relaxed
8	XZ60	5	2	2	2	Relaxed
9	XZ60	5	3	-2	-2	Relaxed
10	XZ60	5	3	-2	6	Relaxed
11	XZ60	5	3	6	-2	Relaxed
12	XZ60	5	3	6	6	Relaxed
13	XZ60	22	1	-2	-2	Relaxed
14	XZ60	22	1	-2	6	Relaxed
15	XZ60	22	1	6	-2	Relaxed
16	XZ60	22	1	6	6	Relaxed
17	XZ60	22	2	2	2	Relaxed
18	XZ60	22	3	-2	-2	Relaxed
19	XZ60	22	3	-2	6	Relaxed
20	XZ60	22	3	6	-2	Relaxed
21	XZ60	22	3	6	6	Relaxed
22	XZ60	13,5	1	2	2	Relaxed
23	XZ60	13,5	3	2	2	Relaxed
24	XZ60	13,5	2	-2	2	Relaxed
25	XZ60	13,5	2	6	2	Relaxed
26	XZ60	13,5	2	2	-2	Relaxed
27	XZ60	13,5	2	2	6	Relaxed
28	XZ60	13,5	2	2	2	Relaxed

100% activated muscles

Simulation Number	Impact Direction	Impact level(G)	Helmet Weight (kg)	Weight COM X-direction (cm)	Weight COM Z-direction (cm)	Activation
29	XZ60	5	2	2	2	100%
30	XZ60	13,5	2	2	2	100%
31	XZ60	22	2	2	2	100%

3.1.2 Refined simulations and results

The contractor has improved the results from the FE model of the neck. Special focus has been on the stresses in the bone. All 196 simulations presented in Halldin et al. (2005) were re-computed with another choice of inclusion criteria for the elements in the vertebral bodies. The elements where stress concentration was seen were excluded. The included elements are shown in grey and the excluded elements are shown in red, Figure 4. A new set of normalized stress calculations are presented in Appendix A and also presented in Interim report 10.

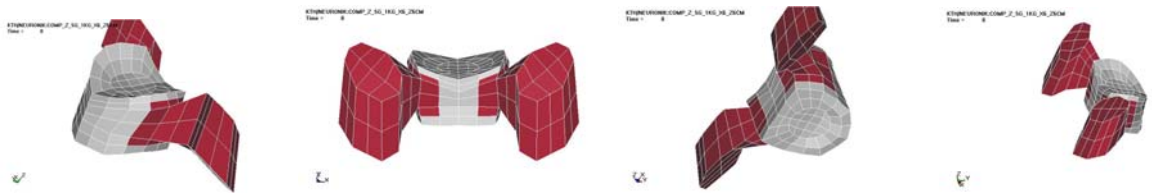

Figure 4. All elements marked with red color were neglected when calculating the risk for fracture in the vertebral bone.

The results have also been analyzed in more detail and the results are presented in Section 3.2.1. The following results are presented:

- BC values (according to Bass et al. 2004).
- Normalized ligament deformation (Halldin et al. 2005).
- Normalized stresses in the compact and trabecular bone (Halldin et al. 2005).

3.1.3 Comparison of relaxed and tensed muscles

In the simulations 1-28 described in Table 2, the relaxed activation scheme was used. The relaxed activation scheme is defined as the minimum constant activation force used to stabilize the head in a gravitational field. The relaxed activation scheme for simulation number 1-28 was presented in Appendix B in Halldin et al. 2005 (Final Phase 2 Report). In Table 3 is just the relaxed activation scheme presented for the neck modeled without helmet.

The tensed activation scheme in simulation 29-31 should be seen as an extreme condition for the neck musculature and is not a physiological condition. The tensed activation is here defined as 100% activation force for the hill-type spring type muscle model used in the KTH neck model. The force generated in each muscle is defined by its cross sectional area and the optimal length, Brolin et al 2005.

Table 3. The relaxed compared to the tensed activation scheme.

Muscle	Relaxed activation	Tensed Activation
Sternocleidomastoid	0%	100%
Longus Cervicis	5%	100%
R.A.Ma.	2%	100%
r.l. and R.A.Mi.	8%	100%
Scalenus	4%	100%
Suboccipital	20%	100%
Semispinalis	8%	100%
Longissimus	7%	100%
Splenius	7%	100%
Levator Scapulae	5%	100%
Trapezius	1%	100%
Interspinous	30%	100%
Hyoid-muscles	2%	100%
Hyoid-muscles	2%	100%

The extensors (the muscles moving the head in posterior direction) are stronger in the human being than the flexors (Coakwell et al. 2004). Therefore, applying 100% activation to all modeled cervical muscles the head will move in extension. To keep the head in up-right position a head rest was modeled when activating all the neck muscles to 100%, see Figure 5.

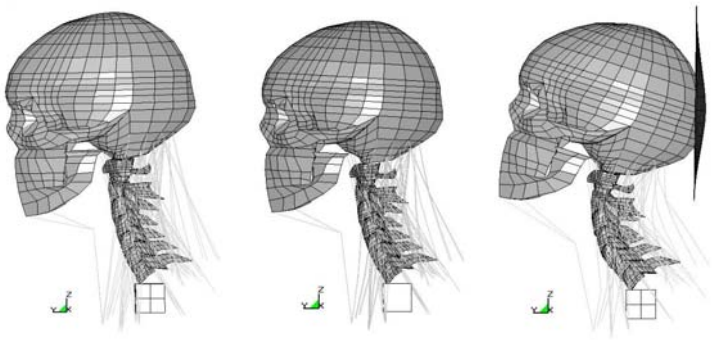

Figure 5: The KTH model for simulation of PMHS impact test (A), sagittal plane impact simulations with no muscle activation (A), relaxed muscle activation (B), and full muscle activation with a head rest (C).

3.1.4 Evaluation of the GUI

The Graphical User Interphase (GUI) uses the results from 28 simulations per load case as presented in Table 2. The Box-Wilson Central Composite Faced (CCF) method is used to perform interpolations between the discrete data points. In order to evaluate the interpolation with the results from the FE model two different helmet configurations was chosen.

It is possible to choose pre-defined helmets with pre defined inertial properties or for the user to design a new helmet with used defined inertial properties. The GUI was evaluated by taking the inertial properties for the pre-defined helmets. The PASGT(1) and the IDHASS(3) helmet was chosen. The masses and centre of gravity for the two helmets are shown in Table 4.

Table 4. The helmet inertial properties used for the GUI evaluation.

Configuration	Helmet	Mass	X-shift	Z-shift
	IDHASS(3)	2,23	3,32	4,15
1	Attachment	1	2	2
	PASGT(1)	1,55	-1,46	5,17
2	Attachment	No	No	No

3.2 Results

3.2.1 Refined simulations and results

The results for all 196 simulations are presented in Appendix A. Below is the results summarized and different comparisons are made.

Figure 6 presents the comparison of the results for different impact directions for the configuration with a 2 kg helmet with CG shifted +2cm in the X- and Z-direction. It can be seen that the Oblique XZ and the Frontal impact results in the highest normalized ligament deformation and the highest Beam Criteria values. Highest vertebral stresses is seen for the lateral direction.

Figure 7 presents the comparison of the computed normalized ligament deformation, beam criteria values and the normalized stresses in the bone for an eight cm CG shift in the X direction. It can be seen that the impacts with a dominating vertical component show the highest changes in the computed values. It should be noted that there is a contradiction for the vertical impact as the beam criteria shows a decrease while the ligament values shows an increase when the CG is shifted forward. The reason for this phenomenon is that the BC value reaches its maximum at 150ms when the neck buckles, Figure 8. Figure 9 shows the animation for the configuration with the CG positioned -2cm in

the X-direction compared with the CG positioned +6cm in the X-direction. The maximum ligament stretch is when the neck bends and reaches maximum flexion at about 250ms, Figure 10.

Figure 11 presents the comparison of the computed normalized ligament deformation, beam criteria values and the normalized stresses in the bone for an eight cm CG shift in the Z direction. It can be seen that the impacts with a dominating horizontal and lateral component show the highest changes in the computed values.

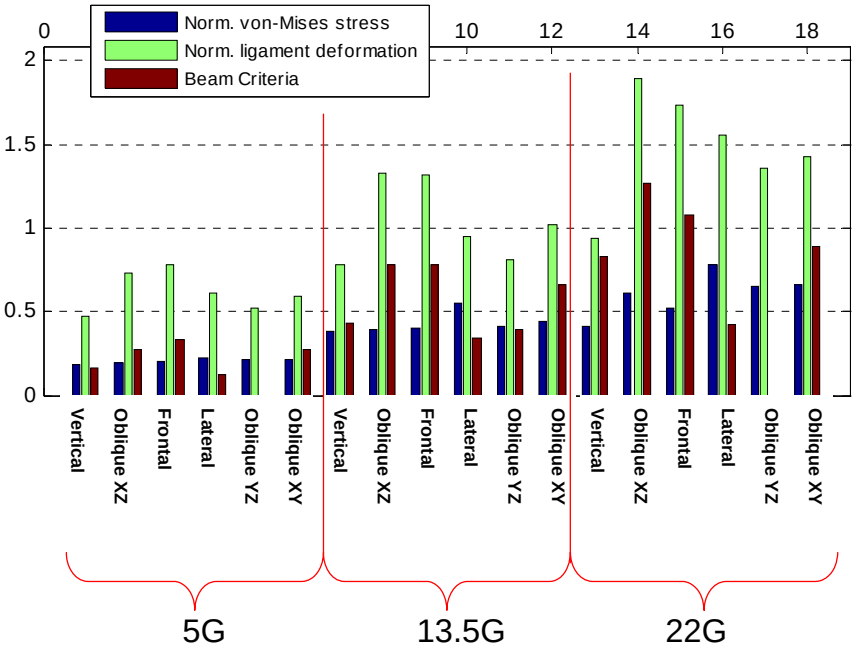

Figure 6. Comparison of the results for different impact directions for the configuration with a 2 kg helmet with CG shifted +2cm in the X and Z-direction.

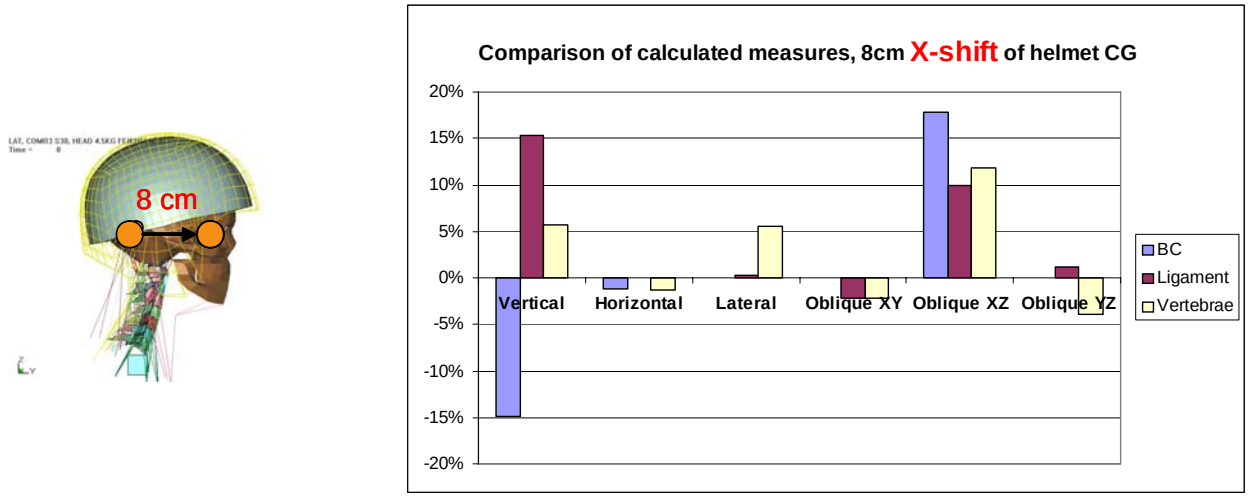

Figure 7. Comparison of the computed normalized ligament deformation, beam criteria values and the normalized stresses in the bone for an eight cm CG shift in the X direction

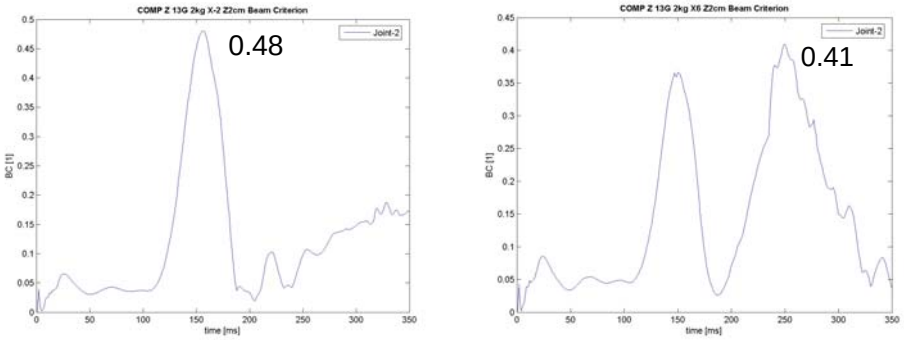

Figure 8. Left: calculated BC values for the 13.5G Vertical Z impact with a 2kg helmet with the CG positioned -2cm and +2cm in the X- and Z-direction, respectively. Left: calculated BC values for the 13.5G vertical impact with a 2kg helmet with the CG positioned +6cm and +2cm in the X- and Z-direction, respectively.

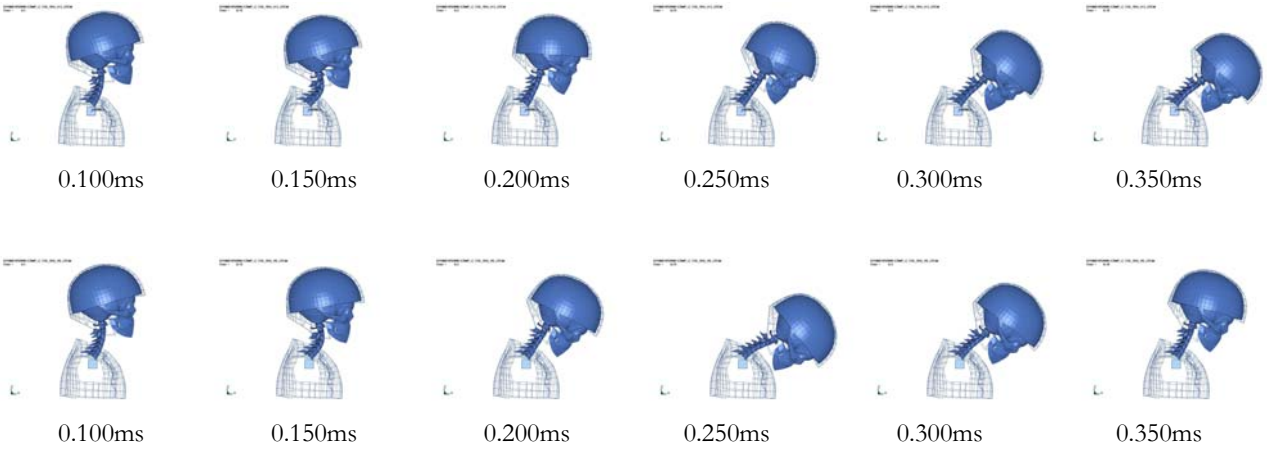

Figure 9. Above: Animation showing the simulation of the 13.5G Vertical Z impact with a 2kg helmet with the CG positioned -2cm and +2cm in the X- and Z-direction, respectively. Below: Animation showing the simulation of the 13.5G vertical impact with a 2kg helmet with the CG positioned +6cm and +2cm in the X- and Z-direction, respectively

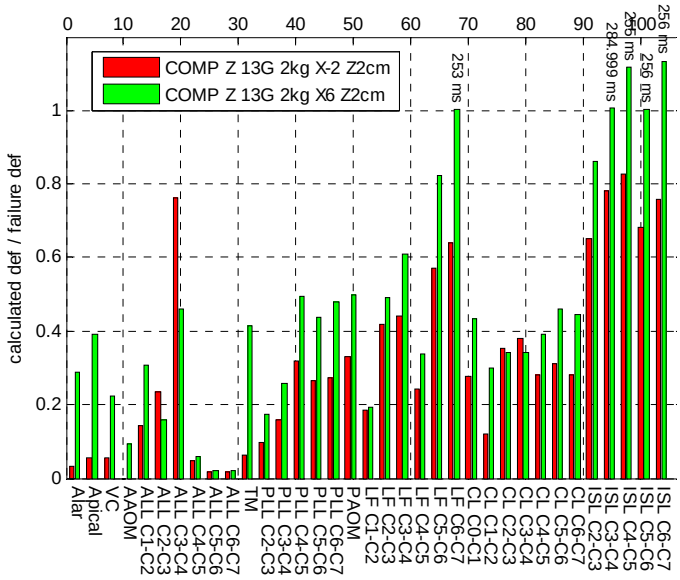

Figure 10. Calculated normalized ligament deformation values for the 13.5G Vertical Z impact with a 2kg helmet with the CG positioned -2cm and +2cm in the X- and Z-direction, respectively, compared with a helmet where the CG is shifted 8cm forward.

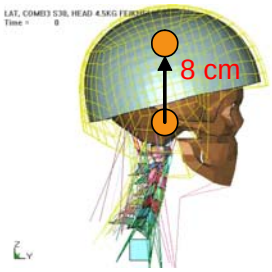

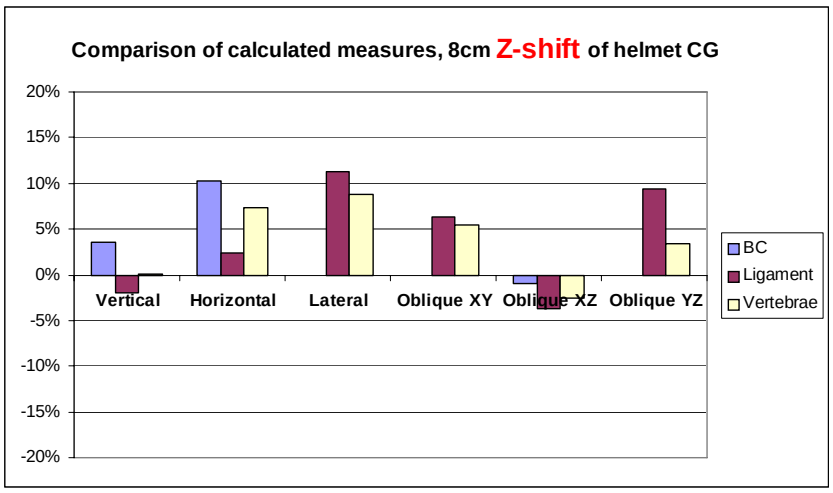

Figure 11. Comparison of the computed beam criteria values, normalized ligament deformation and the normalized stresses in the bone for an eight cm CG shift in the X direction.

Figure 12 presents the changes of the Normalized ligament deformation for an 8cm CG-shift in the X-direction for different impact energies. In this comparison is also 3G-simulations included. The presented values are average calculated changes from comparison of different combinations of helmet CG configurations, See examples from Vertical and Frontal impact in Figure 13 and 14.

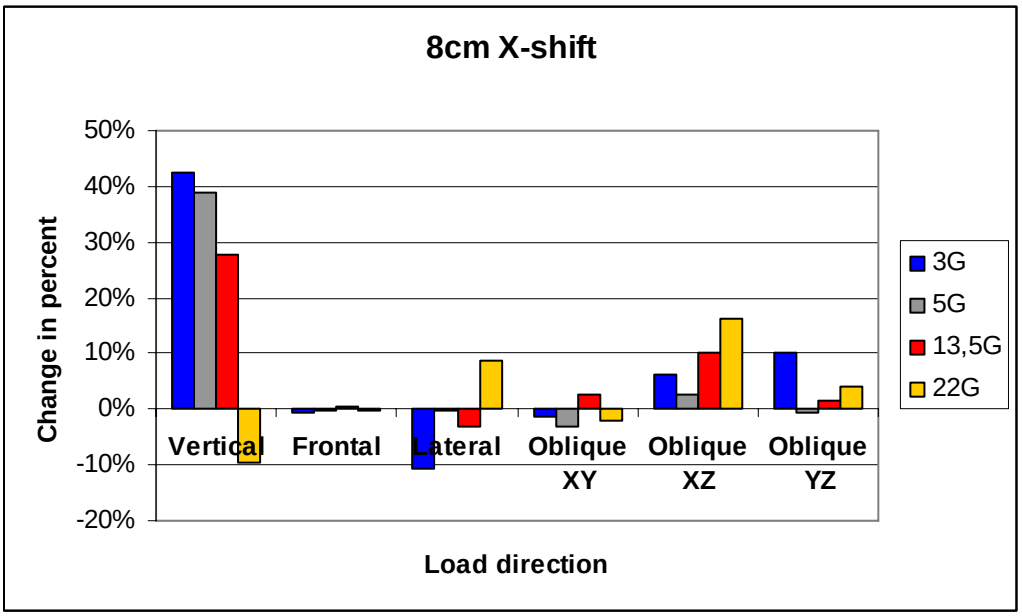

Figure 12. The changes of the Normalized ligament deformation for an 8cm CG-shift in the X-direction for different impact energies

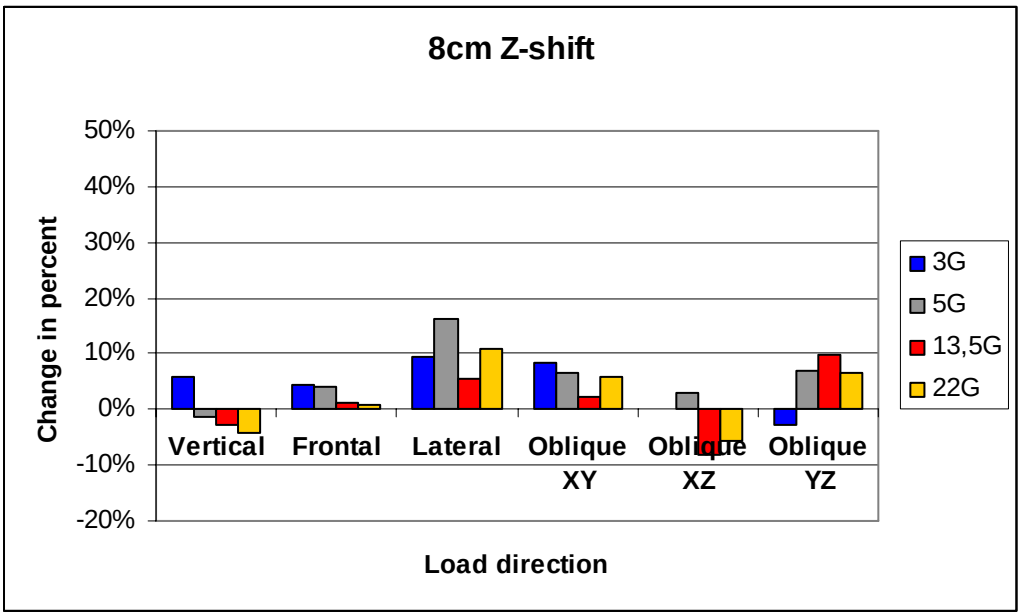

Figure 13. The changes of the Normalized ligament deformation for an 8cm CG-shift in the X-direction for different impact energies

CG shifted 8cm in X-direction		
Helmet Configuration (Impact acceleration; mass of helmet; CG in Z-direction	Ligament with highest def.	Change of ligament deformation
3G; 1kg; Z-2cm	ISL C3-C4	33%
3G; 1kg; Z6cm	ISL C3-C4	32%
3G; 3kg; Z-2cm	ISL C4-C5	46%
3G; 3kg; Z6cm	ISL C4-C5	59%
5G; 1kg; Z-2cm	ISL C4-C5	32%
5G; 1kg; Z6cm	ISL C3-C4	30%
5G; 3kg; Z-2cm	ISL C4-C5	41%
5G; 3kg; Z6cm	ISL C4-C5	53%
13G; 2kg; Z-2cm	ISL C6-C7	28%
13G; 2kg; Z2cm	ISL C6-C7	27%
13G; 2kg; Z6cm	ISL C6-C7	28%
22G; 1kg; Z-2cm	ISL C6-C7	14%
22G; 1kg; Z6cm	ISL C6-C7	10%
22G; 3kg; Z-2cm	ISL C2-C3	-17%
22G; 3kg; Z6cm	ISL C4-C5	-46%

CG shifted 8cm in Z-direction		
Helmet Configuration (Impact acceleration; mass of helmet; CG in X-direction	Ligament with highest def.	Change of ligament deformation
3G; 1kg; X-2cm	ISL C5-C6	10%
3G;1kg; X6cm	ISL C3-C4	9%
3G; 3kg; X-2cm	ISL C5-C6	-12%
3G; 3G; X6cm	ISL C4-C5	17%
5G; 1kg; X-2cm	ISL C3-C4	8%
5G;1kg; X6cm	ISL C3-C4	6%
5G; 3kg; X-2cm	ISL C3-C4	-22%
5G; 3G; X6cm	ISL C4-C5	3%
13G; 2kg; X-2cm	ISL C4-C5	-1%
13G; 2kg; X2cm	ISL C4-C5	-6%
13G; 2kg; 6cm	ISL C6-C7	-2%
22G; 1kg; X-2cm	ISL C6-C7	3%
22G;1kg; X6cm	ISL C6-C7	-1%
22G; 3kg; X-2cm	ISL C6-C7	3%
22G; 3kg; X6cm	ISL C4-C5	-21%

Figure 14. Changes in the calculated normalized ligament deformation for Vertical impacts as function of 8cm CG shift from -2 to 6cm.

CG shifted 8cm in X-direction		
Helmet Configuration (Impact acceleration; mass of helmet; CG in Z-direction	Ligament with highest def.	Change of ligament deformation
3G; 1kg; Z-2cm	ISL C4-C5	0%
3G; 1kg; Z6cm	ISL C4-C5	-1%
3G; 3kg; Z-2cm	ISL C4-C5	-1%
3G; 3kg; Z6cm	ISL C4-C5	-1%
5G; 1kg; Z-2cm	ISL C4-C5	1%
5G; 1kg; Z6cm	ISL C4-C5	1%
5G; 3kg; Z-2cm	ISL C4-C5	-3%
5G; 3kg; Z6cm	ISL C4-C5	0%
13G; 2kg; Z-2cm	ISL C6-C7	-2%
13G; 2kg; Z2cm	ISL C6-C7	1%
13G; 2kg; Z6cm	ISL C6-C7	2%
22G; 1kg; Z-2cm	ISL C6-C7	0%
22G; 1kg; Z6cm	ISL C6-C7	1%
22G; 3kg; Z-2cm	ISL C6-C7	-3%
22G; 3kg; Z6cm	ISL C6-C7	2%

CG shifted 8cm in Z-direction		
Helmet Configuration (Impact acceleration; mass of helmet; CG in X-direction	Ligament with highest def.	Change of ligament deformation
3G; 1kg; X-2cm	ISL C4-C5	2%
3G;1kg; X6cm	ISL C4-C5	2%
3G; 3kg; X-2cm	ISL C4-C5	7%
3G; 3G; X6cm	ISL C4-C5	7%
5G; 1kg; X-2cm	ISL C4-C5	2%
5G;1kg; X6cm	ISL C4-C5	1%
5G; 3kg; X-2cm	ISL C2-C3	5%
5G; 3G; X6cm	ISL C4-C5	8%
13G; 2kg; X-2cm	ISL C6-C7	-1%
13G; 2kg; X2cm	ISL C6-C7	2%
13G; 2kg; 6cm	ISL C6-C7	3%
22G; 1kg; X-2cm	ISL C6-C7	0%
22G;1kg; X6cm	ISL C6-C7	1%
22G; 3kg; X-2cm	ISL C6-C7	-2%
22G; 3G; X6cm	ISL C6-C7	3%

Figure 15. Changes in the calculated normalized ligament deformation for Vertical impacts as function of 8cm CG shift from -2 to 6cm.

The results for the Rear end impacts were excluded as the boundary condition for the vertebral column resulted in unrealistic motion of the neck. The boundary condition between the helmet and the model of the thorax results in a sliding of the helmet against the thorax which is believed to be unrealistic, see Figure 16. The loss of muscle volume in the spring muscle model can also result in this unrealistic hyper extension motion.

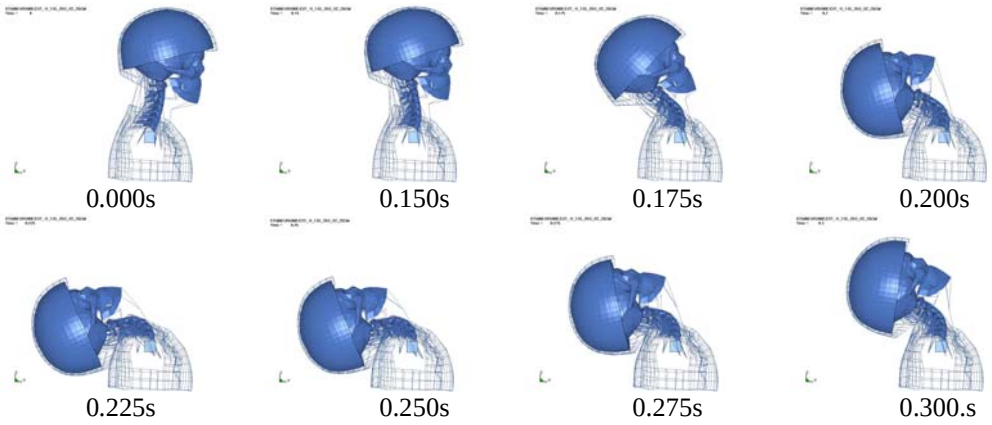

Figure 16. Simulation of a 13.5G rear end impact. The unrealistic motion of the neck is seen between 200 and 250ms as the boundary condition between the helmet and the thorax result in a sliding between the helmet and the thorax.

3.2.2 Comparison of relaxed and tensed muscles

Figure 17 shows the kinematics for the relaxed and the tensed muscle activation for the OBL_XZ: 13.5G: X+2cm: Z+2cm. It was shown that the model with tensed muscles can prevent the chin from impacting the chest at a 13.5G impact.

The ligament deformation is reduced by 17% (Figure 18), the BC value by 22% (Figure 19) and the stress in the vertebrae is increased by 2% (Figure 20). The results for the Oblique_XZ impacts are summarized in Figure 21.

The results for the Vertical, Frontal and Oblique_XY are presented in Figure 22, Figure 23 and Figure 24. The tensed activation result in a reduction of the calculated ligament deformation for all impact directions and impact energies. The BC values are reduced for the 13.5G and 22G pulses but are increased for the 5G impacts.

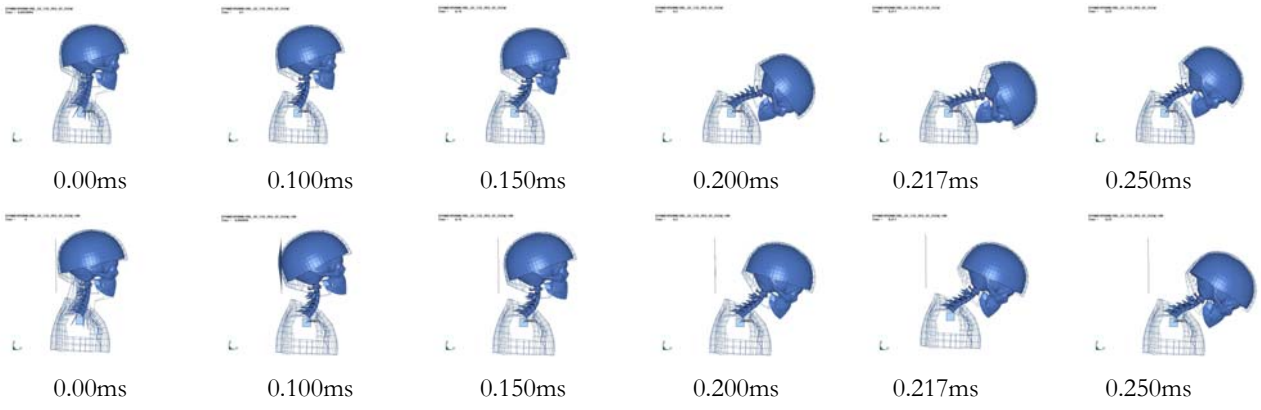

Figure 17. Above: Relaxed activation, Bellow: Tensed activation for the 13.5G Oblique_XZ impact. The helmet mass is 2 kg and the CG is positioned +2cm and +2cm, in the X and Z direction, respectively.

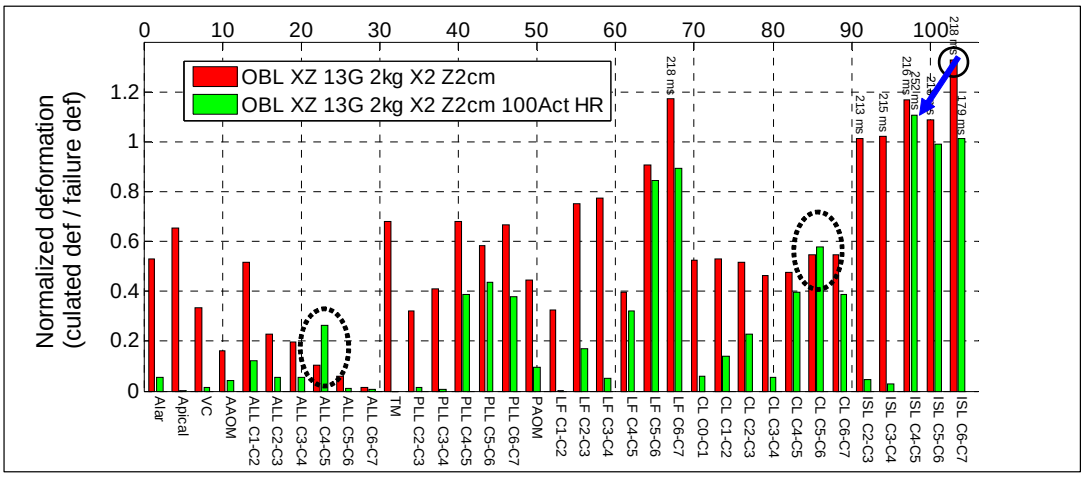

Figure 18. **Comparing the normalized ligament deformation for the Oblique XZ: 13.5G: X+2cm: Z+2cm simulation with relaxed (Red) and activated musculature (Green). The blue arrow shows the decrease of the normalized ligament deformation. The dotted circles show the ligaments that sustain an increased ligament deformation as the muscles are tensed.**

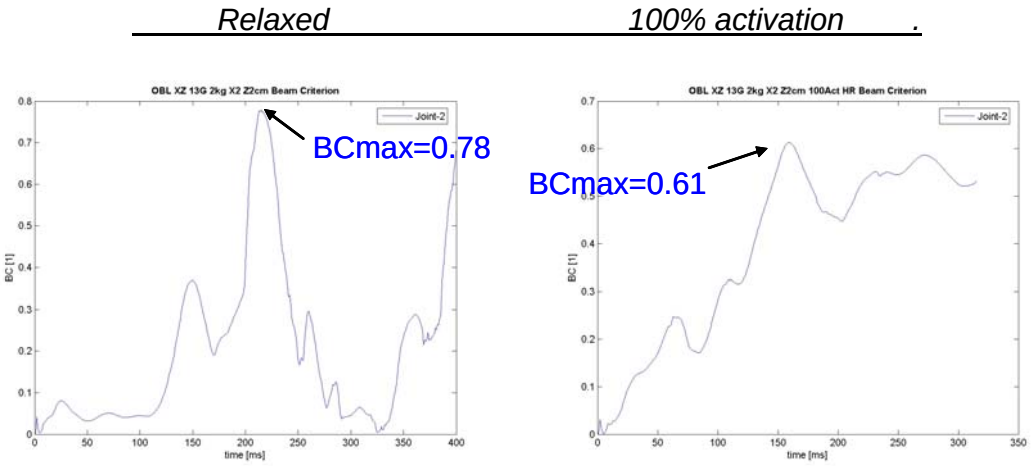

Figure 19. **Calculated beam criteria values for the Oblique XZ: 13.5G: X+2cm: Z+2cm simulation with relaxed and tensed muscle activation.**

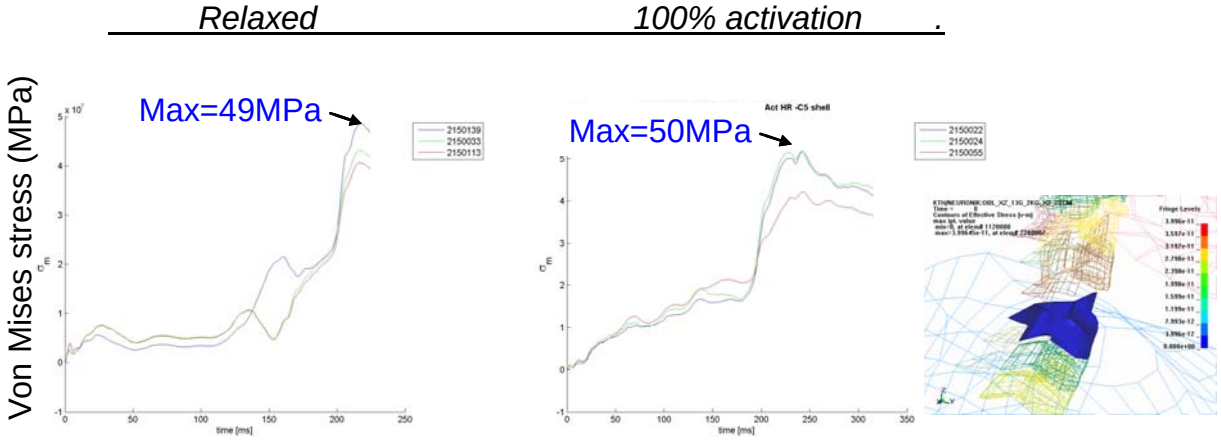

Figure 20. **Computed von Mises stress for the Oblique XZ: 13.5G: X+2cm: Z+2cm simulation with relaxed and tensed muscle activation.**

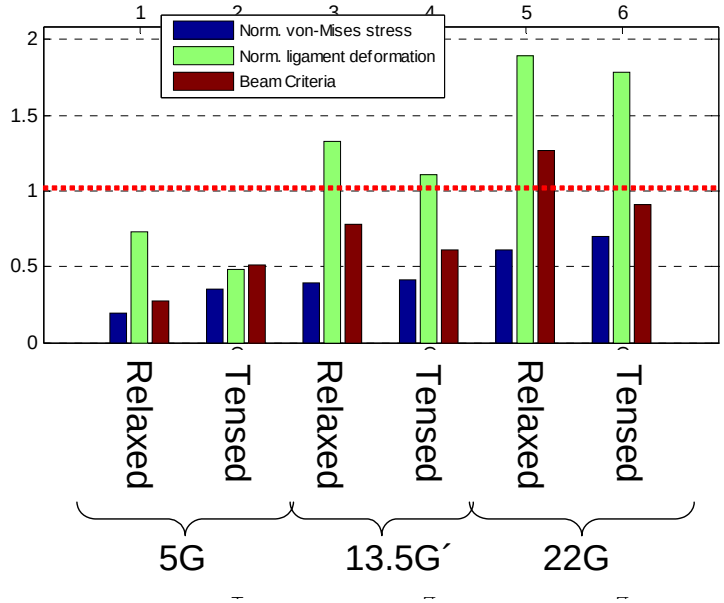

Figure 21. **Comparison of the calculated normalized von Mises stress, normalized ligament deformation and Beam Criteria values for the Oblique XZ: 5G, 13.5G and 22G: X+2cm: Z+2cm simulations with relaxed and tensed muscle activation.**

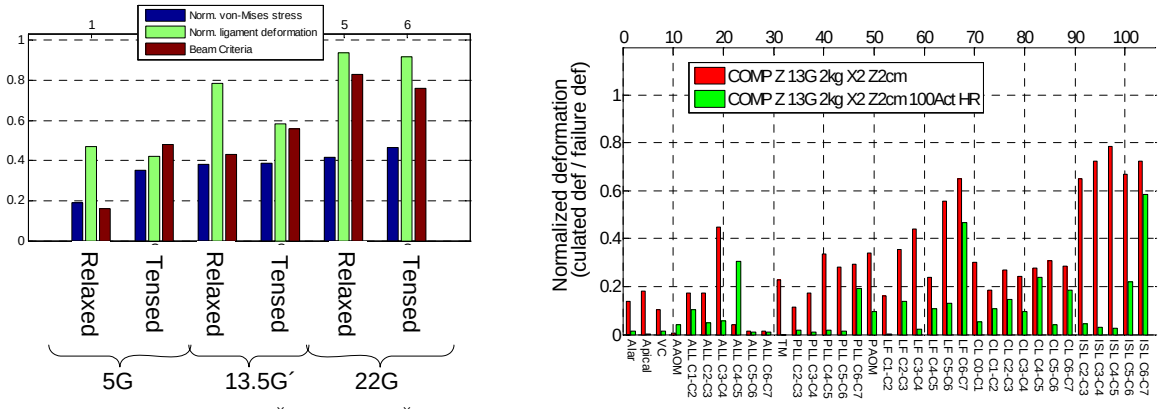

Figure 22. ***Left:*** **Comparison of the calculated normalized von Mises stress, normalized ligament deformation and Beam Criteria values for the Vertical Z: 5G, 13.5G and 22G: X+2cm: Z+2cm simulations with relaxed and tensed muscle activation.** ***Right:*** **Comparing the normalized ligament deformation for the Vertical Z: 13.5G: X+2cm: Z+2cm simulation with relaxed (Red) and activated musculature (Green).**

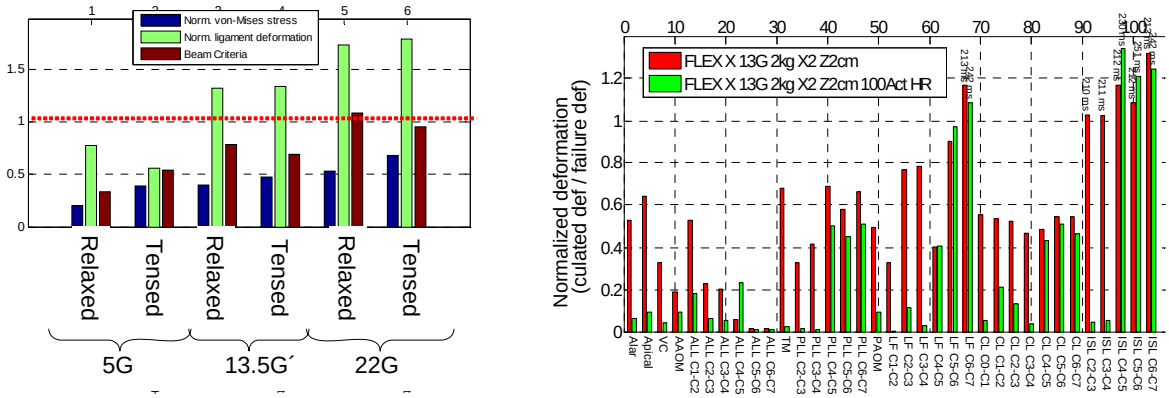

Figure 23. ***Left:*** **Comparison of the calculated normalized von Mises stress, normalized ligament deformation and Beam Criteria values for the <u>Frontal X</u>: 5G, 13.5G and 22G: X+2cm: Z+2cm simulations with relaxed and tensed muscle activation.** ***Right:*** **Comparing the normalized ligament deformation for the <u>Frontal X</u>: 13.5G: X+2cm: Z+2cm simulation with relaxed (Red) and activated musculature (Green).**

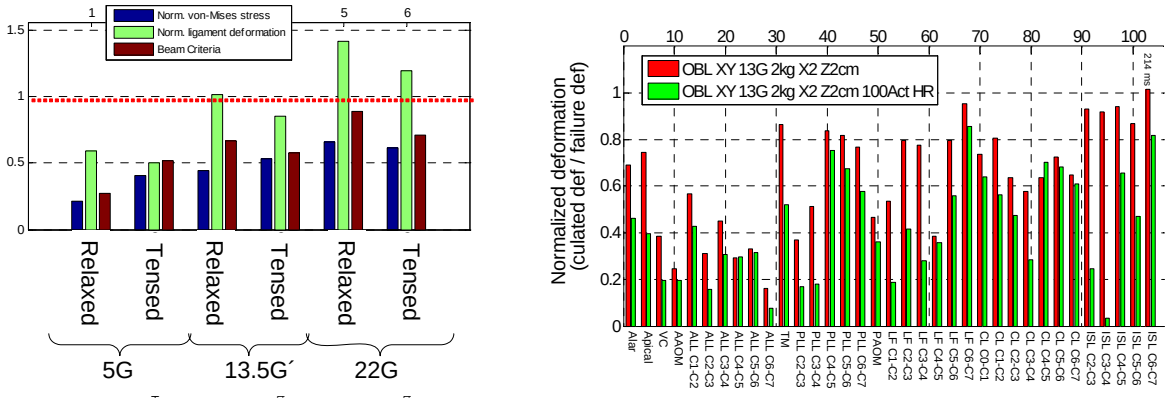

Figure 24. ***Left:*** **Comparison of the calculated normalized von Mises stress, normalized ligament deformation and Beam Criteria values for the <u>Oblique XY</u>: 5G, 13.5G and 22G: X+2cm: Z+2cm simulations with relaxed and tensed muscle activation.** ***Right:*** **Comparing the normalized ligament deformation for the <u>Oblique XY</u>: 13.5G: X+2cm: Z+2cm simulation with relaxed (Red) and activated musculature (Green).**

Figure 25 summarize different changes in the simulations and shows the computed maximum normalized stress in bone and maximal normalized deformation in the ligaments and the beam criteria for 13.5G pulses in the Vertical, frontal, Oblique XZ and Oblique XY.. The following comparisons were made.

- 8cm shift of the 2kg helmet CG in the X-direction
- 8cm shift of the 2kg helmet CG in the Z-direction
- Increasing the mass of the helmet by 1 kg (From 2kg to 3kg).
- Increasing the muscle activation from approximately 5% to 100% (13.5G; 2kghelmet; X+2cm; Z+2cm).

The results can be summarized with:

1. Shifting the CG forward does affect the results especially for the vertical and the oblique XZ loading.

2. Adding 1kg mass shows small effect on the computed values except for the BC values in vertical impacts. Ligament deformation and vertebral stress do not increase more than 8% for any impact direction.
3. Activating the muscles does affect all directions significantly in the 13.5G impact.

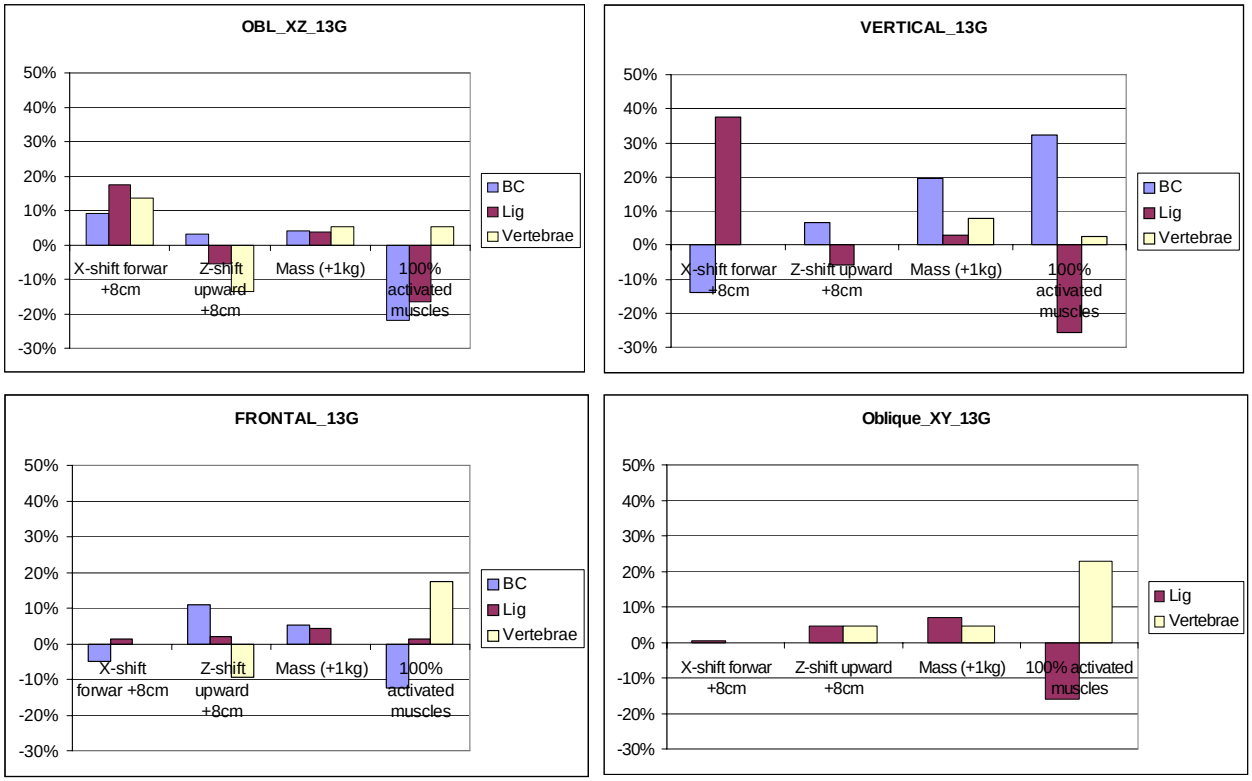

Figure 25. The figure summarizes the change of the computed Beam Criteria (BC), normalized ligament deformation (Lig) and the normalized vertebral stresses (Vertebrae) in percent. The bars compare an 8cm X-shift of the CG, 8cm Z-shift of the CG, an increase of the helmet mass from one to two kg and the change from relaxed to activated muscle activation. The figures shows from top left to bottom right, Oblique_XZ, Vertical_Z, Frontal_X and Oblique_XY.

3.2.3 Evaluation of the GUI

The GUI uses the discrete result points from 28 simulations per load case. Between the extreme values is the Central Composite Faced (CCF) method used. Table 5 shows the how well the CCF method works. The interpolation method between the discrete points works well for all load cases except for the Oblique_YZ, 5G and13.5G pulses.

Table 5. Evaluation of the GUI. Two different helmet configurations were studied. In the right column is the differences presented in percentage.

	Ligament strain		
	KTH Neck Model	GUI	Difference (%)
Helmet: IDHASS(3) + 1kg attachment			
Helmet mass: Xshift:Zshift Attachm. mass: Xshift: Zshift	2.23kg: 3.32cm: 4.15cm 1kg: 2cm: 2cm	2.23kg: 3.32cm: 4.15cm 1kg: 2cm: 2cm	
Vertical_Z_22G	1,14	1,13	-0,01
Vertical_Z_13G	0,77	0,80	0,04
Frontal_X_13G	1,37	1,36	0,00
Frontal_X_22G	1,81	1,83	0,01
Frontal_X_5G	0,77	0,80	0,04
Lateral_Y_13G	0,95	1,03	0,09
Lateral_Y_22G	1,75	1,74	-0,01
Lateral_Y_5G	0,66	0,69	0,05
Oblique_XY_13G	1,07	1,09	0,02
Oblique_XY_22G	1,51	1,55	0,03
Oblique_XY_5G	0,63	0,62	-0,02
Oblique_XZ_13G	1,35	1,40	0,04
Oblique_XZ_22G	1,94	2,03	0,04
Oblique_XZ_5G	0,72	0,77	0,07
Oblique_YZ_13G	0,84	0,98	0,17
Oblique_YZ_22G	1,46	1,48	0,01
Oblique_YZ_5G	0,60	0,54	-0,10
Helmet: PASGT(1)			
Helmet mass: Xshift:Zshift Attachment mass: Xshift: Zshif	1.55kg: -1.46cm: 5.17cm -	1.55kg: -1.46cm: 5.17cm -	
Vertical_Z_22G	0,68	0,62	-0,09
Vertical_Z_13G	0,95	1,00	0,05
Frontal_X_13G	1,28	1,25	-0,02
Frontal_X_22G	1,70	1,71	0,01
Frontal_X_5G	0,77	0,78	0,02
Lateral_Y_13G	0,92	0,93	0,01
Lateral_Y_22G	1,50	1,51	0,01
Lateral_Y_5G	0,62	0,63	0,01
Oblique_XY_13G	1,00	0,99	-0,01
Oblique_XY_22G	1,44	1,45	0,01
Oblique_XY_5G	0,60	0,60	0,00
Oblique_XZ_13G	1,21	1,17	-0,03
Oblique_XZ_22G	1,78	1,72	-0,03
Oblique_XZ_5G	0,70	0,69	-0,01
Oblique_YZ_13G	0,82	0,87	0,07
Oblique_YZ_22G	1,31	1,34	0,02
Oblique_YZ_5G	0,52	0,50	-0,04

4 Task C: Development of an anatomical correct representation of the musculature

As a part of the refinement and further development of the KTH neck model the cervical musculature is being remodeled with anatomical correct geometry and continuum mechanical properties. Most cervical models of today use spring-elements as muscles. A detailed solid-element muscle model will

add properties such as tissue inertia and compressive stiffness into the model and should therefore better predict injuries to the cervical tissues than a spring muscle model.

The deep and superficial cervical muscles were modeled with solid finite elements. The 3D geometry was digitized from MR images of 50th percentile males. The MR images were segmented and interpolated to generate a three-dimensional surface for each muscle. The muscle surfaces were positioned relative to the FE KTH neck model [Brolin et al. 2005] in line with anatomical data from the literature and adjusted to a normal lordosis of a sitting person before meshing. The passive properties were modeled using solid elements and a non-linear, viscoelastic continuum material model. The active properties were modeled separately using discrete elements and a Hill-type material model. The material modeling was validated for a tensile test of a rabbit muscle for strains below 30%. The model is described in more detail in earlier interim reports, see Section 5.

4.1 Muscle Modeling

22 pairs of muscles have been included into the model, 26, as well as rigid body mastoid processes and a hyoid bone for boundary conditions and muscular insertions. The hyoid bone is constrained to the 3rd cervical vertebra and the mastoid process to the skull.

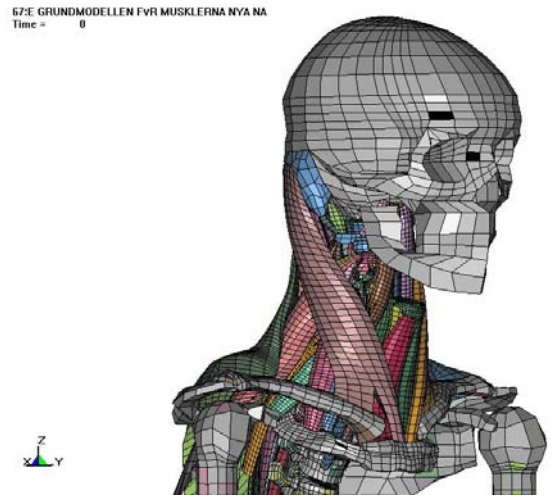

Figure 26 The KTH neck model with 22 pairs of solid muscles, including the Sternocleidomastoid, the trapezius, the mastoid processes and the hyoid bone.

The muscles were added from the innermost layer and out. Innermost are the suboccipital muscles and the erector spinae muscles, multifidus and semispinalis cervicis, Figure 27.

The posterior side of the muscle model includes the semispinalis-; splenius-; and the longissimus muscles as well as the Iliocostalis cervicis and levator scapula enveloped by the trapezius muscle, Figure 28. The trapezius muscle is divided into a superior and an inferior part.

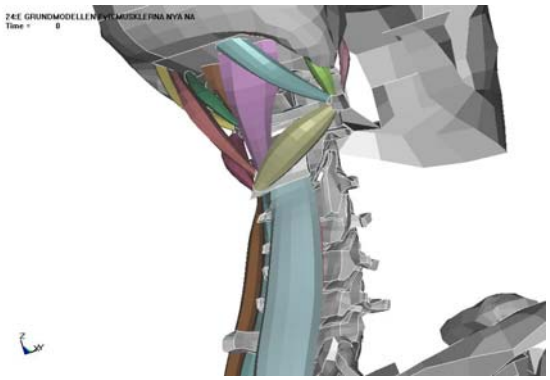

Figure 27 The deep laying suboccipital and erector spinae muscles.

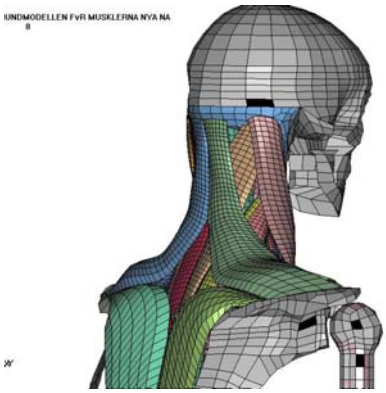

Figure 28 The Trapezius muscles divided into a superior and inferior part

At the anterior side the muscle model includes the Longus Capitis muscle and Longus Colli, divided into a superior, an inferior and a longitudinal part, and the three Scalene muscles, Figure 29. The infra hyoid muscles, sternohyoid and sternothyroid, are modeled together as one entity and the supra hyoids are modeled with discrete elements, Figure 30.

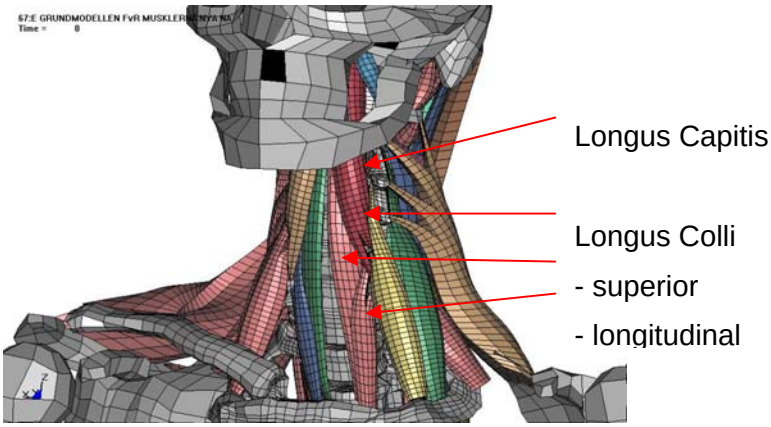

Figure 29 The anterior side of the KTH neck model with the Longus Colli muscle divided into the superior, inferior and longitudinal part and the Scalenes and Levator Scapula

To support the anterior muscles and fill the space between the Longus Colli and the hyoid muscles a combined trachea and esophagus is included in the model. It is modeled as an elastic cylinder attached to the hyoid bone at top and the sternum at the lower end, Figure 30.

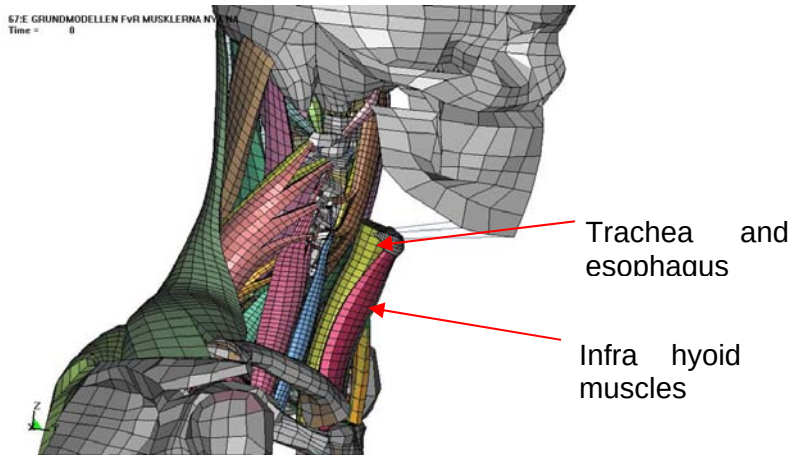

Figure 30 Included in the KTH neck model is the trachea and esophagus as support to the cervical muscles; they are modeled together as a cylinder.

As a result during the modeling attempts it was found that Ligamentum Nuchae was needed to prevent the posterior muscles from buckling in head extension. Also a skin was included in the model to hold the sternocleidomastoid in place, Figure 31.

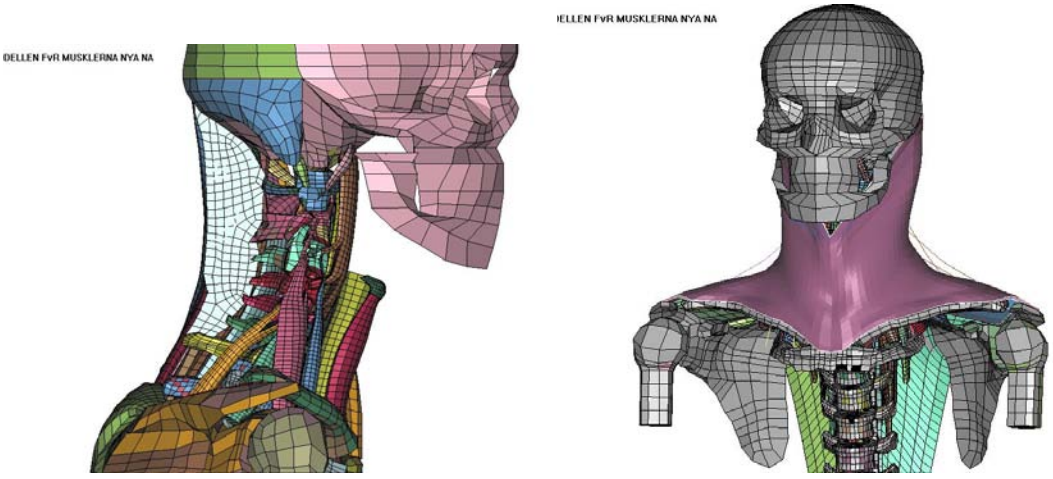

Figure 31 The KTH neck model with a shell element Ligamentum Nuchae and a solid element skin added to give support to the cervical muscles.

4.2 Validation and evaluation of the continuum muscle model

The solid muscle model was evaluated by comparing its behavior during impact loading with experimental data and that of the existing spring muscle model. The impact directions studied were:

- oblique XZ
- rear-end
- lateral and
- oblique XY

4.2.1 Oblique XZ

The model was loaded with a 22G acceleration pulse in the Oblique XZ 60 degree direction as described in Halldin et a. 2004. The oblique XZ pulse resulted in a head neck flexion shown in Figure

32. This was a high-energy pulse of 22G performed on post mortem subjects (PMS) by Bass et al 2004. The same pulse was used for the solid and spring muscle models and the models were passive.

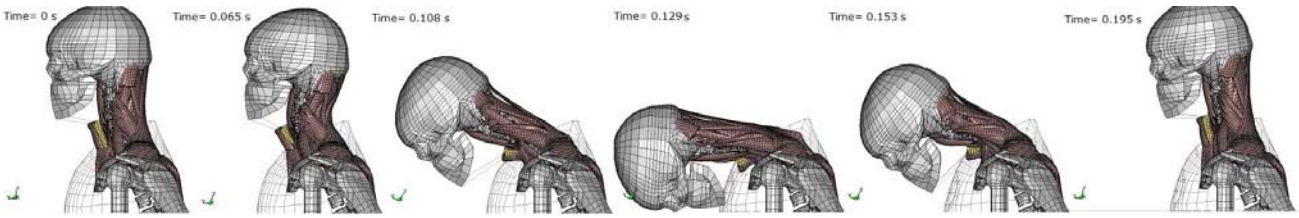

Figure 32 The KTH model with solid muscles when subjected to an oblique XZ 22G pulse.

The kinematics of the head relative T1 for the solid model was, as seen in Figure 33, similar to that of the old spring muscle model but with slightly more restricted motions.

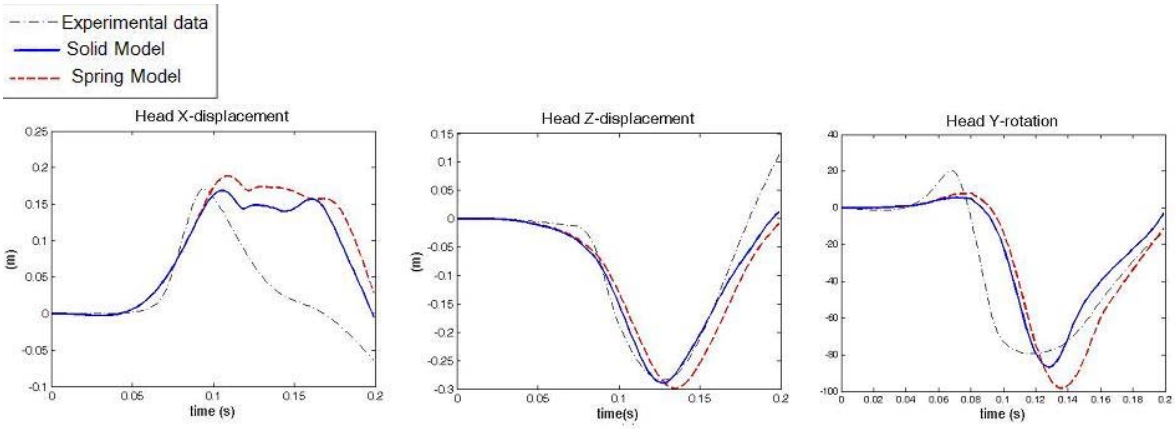

Figure 33 Kinematics of the head relative T1 for an oblique XZ impact of 22G with a passive musculature, X displacement, Z displacement and Y rotation.

4.2.2 Rear-end

The rear-end impact was chosen to be a low-energy pulse of 4G, similar to an experiment performed on volunteers, Halldin et al 2004.. Since this experiment included volunteers that activated their musculature the contractile elements in the model were activated according to a pattern developed for extending motions. However the activation was not optimized for either the solid or the spring model. Therefore are the results not compared with experimental data but only in-between the two muscle models. For evaluation of the influence of activation also passive musculature were simulated for both models. The results show that the solid muscle model stiffens the head in extension and the motion is decreased compared with the spring muscle model. The difference between solid and spring muscle elements seemed to be larger than the effect of an activated musculature. The maximal extension of the head for both models is seen in Figure 34 and the kinematics of the head relative T1 is seen in Figure 35.

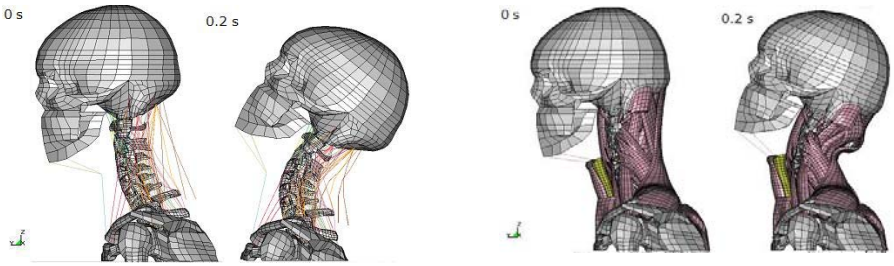

Figure 34 The KTH model subjected to a rear-end low energy pulse resulting in an extension. The spring muscle modeled allows the head to move

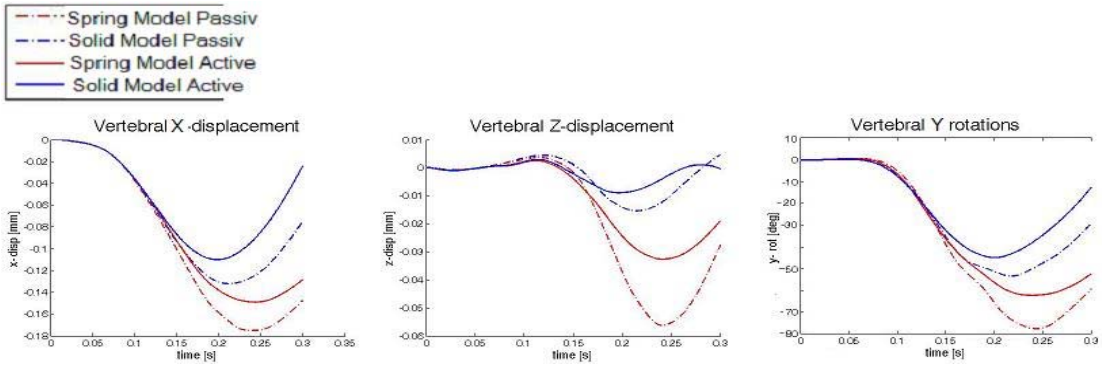

Figure 35 Kinematics of the head relative T1 for a rear-end pulse of 4G, with activated and passive musculature (dashed lines).

4.2.3 Lateral

Also the lateral impact was a 7G pulse from volunteer experiments performed by Ewing et al (1977). The resulting kinematics of the head relative T1 is seen in Figure 36 and Figure 37. No activation was used in this simulation.

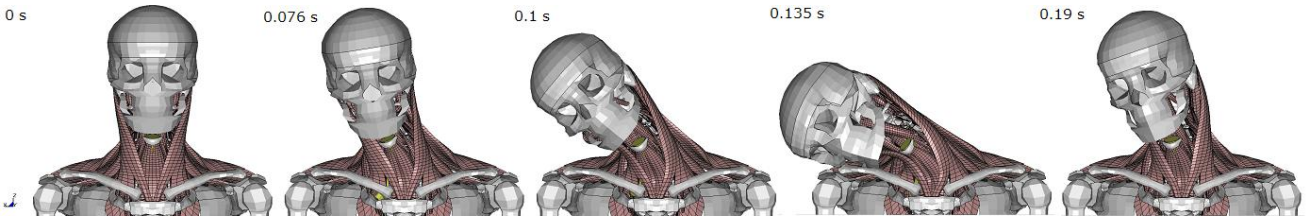

Figure 36 The kinematics of the passive solid muscle model for a lateral impact of 7G.

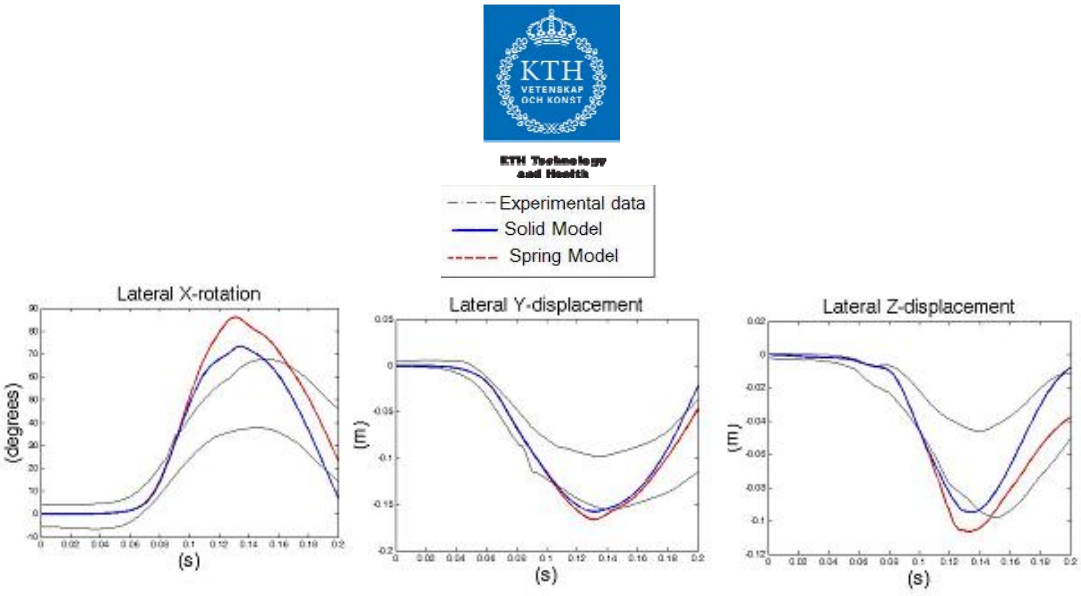

Figure 37 Kinematics of the head relative T1 for X rotation, Y displacement and Z displacement, for a lateral impact, experimental corridors from volunteers.

4.3 Results - Task C

The KTH neck model with continuum musculature generates a motion pattern that takes the compressive stiffness, tissue inertia and the material properties of non-linearity and viscosity into account. The new continuum muscle model stabilized the vertebral column for the tested impact directions and thereby reduced the stresses and strains in vertebrae and ligaments. The continuum muscle model showed the largest effect in the rear end impact direction compared to the spring muscle model.

4.4 Conclusions and future work - Task C

For all analyzed load cases the solid musculature supported and stiffened the behavior of the vertebral column. The stresses and ligament deformation was reduced and the kinematics was stiffer for the solid muscle model. The largest effect was seen for the rear end impact as the compressed muscles restrained the motion

The future development of the continuum muscle model will concern the boundary conditions from surrounding tissues, the ability of the active muscle tissue to contract in compression and thereby prevent it from buckling and to combine the active springs and the passive solid elements.

The present version of the model does work for the load cases tested above and will especially add boundary conditions for the extending motions compared to the spring muscle model.

5 Discussion

The KTH FE model of the cervical spine has been used to investigate seven impact scenarios, (frontal, rear end, lateral, vertical, and oblique impacts in the horizontal plane, frontal plane, and sagittal plane.), three impact severities (5, 13.5 and 22 G), three helmet masses (1, 2 and 3 kg), and nine locations of the Center of Gravity of the helmet (offset relative to the CG of the head with -2, 2, and 6 cm in the superior/inferior and anterior/posterior directions). The output from the model has been ligament deformation, stresses in the bone, pressure in the cervical disc and computed forces and moments in the lower part of the neck to calculate the Beam Criteria values (Bass et al. 2004).

The model has in a previous report (Halldin et al. 2004) been compare with volunteer tests in rear end impacts, pure vertical, Frontal, Lateral and Oblique XY impacts and compared to cadaver test data in the Olique XZ direction. The kinematical correlation with the experiments has been good for all load cases except the Oblique XY impact. The model has not been validated for the Olique YZ impact.

The prediction of injury to the ligaments was validated against the cadaver experiments by Bass et al 2004, presented in Halldin et al 2005. This result together with previous results where the KTH neck model injury prediction correlated well to volunteer experiments by Ewing et al. (1976) increases the reliability of the used injury prediction method for ligament rupture. The injury thresholds (125MPa in tension and 200MPa in compression) used for the stresses in the vertebrae has not been validated against cadaver tests. The relative differences between the computed/calculated normalized ligament deformation, BC and vertebral stress shows realistic characteristics for all load directions. A ligament injury to the cervical spine is normally an AIS1 injury while a vertebral fracture is an AIS2+ injury. A BC value of one predicts 50% risk of an AIS2+ injury. For all impacts studied is the computed normalized ligament deformation lower than the BC values, that are lower than the normalized vertebral stresses.

The version of the KTH neck model used for the GUI simulations is robust for all load cases except for the 13.5G and 22G rear end impacts. The reason is a combination of the stiff thorax and the spring muscle model used in the present version of the KTH neck model. It is believed that a 3D solid representation of the musculature would prevent the neck from the hyperextension seen in rear end high energy impacts. The first simulations show optimistic performance of the new continuum muscle model.

In the load cases most similar to helicopter crashes (Vertical, Oblique_XZ and Flexion) the model do predict injuries to the lower region in the cervical spine. This is supported by a study by Shanahan and Shanahan (1989) who investigated the injury outcome from helicopter crashes 1979-1985. Injuries to the lower cervical spine was also seen in an experimental study by Bass et al. 2004 where 36 cadavers were tested situations similar to a typical helicopter accident (Oblique XZ 60 degree impact).

The results in terms of risk associated with the helmet CG location for the different impact directions found in this study correlates well to what has previous been published. The vertical impact direction (+Z) is the most frequently studied loading for investigations of the injury risks associated with head supported mass. The vertical impact is also the most difficult to study and generalize as the head and neck complex is very sensitive for CG shifts around the stiffest axis of the vertebral column. The results from the model exemplify this as the changes of the calculated ligament deformation are very much dependent on several parameters such as CG-shift, helmet mass and impact energy (as seen in Figure 14). So, it is therefore not recommended to use a 2D risk-curve with the mass on one axis and the CG shift on the other without take the load pulse into account.

The vertical impact shows the lowest BC and normalized ligament deformation values. This result correlates well to what was found in the case study by Shannon and Mason (1997) where they analyzed 357 rotary-wing accidents.

Ashrafiuon et al (1997) have performed computer simulations to evaluate the effect of weight and CG location of helmets and head supported devises. They used the Articulated Total Body (ATB) model to simulate manikin and human subjects. The ATB model is made of rigid bodies with joint properties and an option to model the neck as a deformable body was used. This study considered five impact conditions with offset from the vertical and horizontal impact. Their results showed varied effect of the CG location based on the impact condition. For vertical impacts they stated that a backward shift of the CG generally decreased neck forces and moments, which is supported by this study. Also, the forces and moments decreased as the CG moved downwards.

The present results from the KTH neck model include both a pure vertical loading and an oblique sagittal plane impact that seem to contradict the results by Ashrafiuon et al. (1997). The KTH neck model shows reduced BC values as well as ligament deformation values, for most of the helmet masses and impact energies, with increasing vertical position of the helmet CG. However, Ashrafiuon et al. (1997) measured the forces and moments at the occipital condyles and the presented BC values as well as the normalized ligament deformations origin from the lower cervical spine. The deformations of the ligaments in the upper cervical spine increase when the CG is shifted upwards, Figure 34, which is in line with the study by Ashrafiuon et al. (1997). Hence, it can be concluded that shifting the CG upwards reduces the risk for injuries to the lower neck while it increases the risk for injuries to the upper neck. This conclusion was confirmed by comparing the results from a similar study by Manoogian et al. 2005, where they used a rigid body MADYMO neck model. Manoogian presented Nij values for the upper neck and BC values for the lower neck. The results from the MADYMO model showed the same changes in injury risk for the vertical and oblique XZ loading as the KTH neck model.

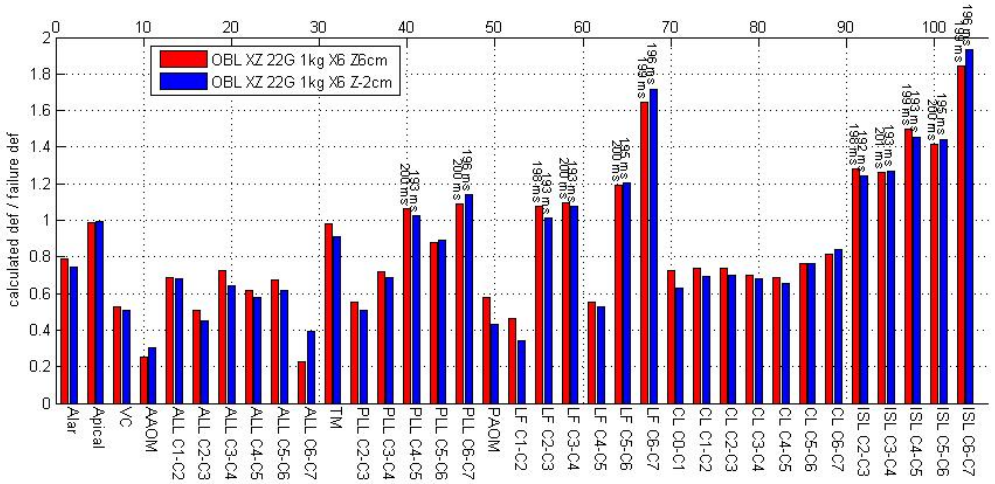

Figure 34. Normalized ligament deformation values from oblique XZ simulations. The red bars show the CG shifted 6cm upwards and the blue bars show the CG shifted 2cm downwards.

The ATB model has been used in another study by Lee et al (1991) of helmet weight, helmet CG and a protective neck air bag for simulation of seat ejections. Among other results they showed that anterior position of the CG had large effects on head deflection. This is also seen in the results from the frontal and oblique XZ impacts simulations with the KTH neck model. Interestingly, only adding helmet mass had little effect on the head deflection angles.

The model of the cervical spine would need a 3D representation of the musculature. The intention was to use the new 3D representation of the muscles in the model. The model that is presented in this report and in several interim reports is under evaluation and is right now undergoing a validation process.

The level of muscle activation has earlier been shown to influence the neck injury risk (Brolin et al. 2005). This has also been discussed in the review article by Green (2003). In Halldin et al. (2005) the activation scheme called *tensed* activation was defined as the maximum activation that can be tuned for the present KTH neck model in order to reach equilibrium for the head in a gravitational field. However, the large extensor, Trapezius, is only activated by 30-33%, since the extensors are much stronger than the flexors (Coakwell et al. 2004). Therefore, the *tensed* activation may not be representative for a person that has the possibility of activating her or his muscle a hundred percent. When analyzing the KTH neck model with full activation the head will, because of the stronger extensors, start to rotate backwards. This can be seen in high speed movies on volunteer tests that the person that is aware of the impact tend to activate his or her muscles so much that the head is pressing against the headrest (National Crash Survival Data Bank, NCSDB). It was therefore decided to run the model with 100% activation for all muscle springs in the model and to add a head rest. It should be noted that the relaxed and tensed (100%) muscle activation is two extreme activation schemes. It is not the authors believe that the activation during an impact can be constant at 100%. The comparison is not a perfect judgment how the relaxed and tensed activation differs as the initial position of the head is dependent on the activation scheme. The different initial condition is shown as the head has different initial rotation from the different activation of the neck musculature. This will effect following kinematics of the cervical spine. However, this fact does not explain the significant influence of the muscle activation. It is suggested that the GUI is complemented with an option where the user can choose if the person is aware or unaware of the accident.

6 Deliverables

The following scientific personnel have participated in the project: MD PhD Hans von Holst, PhD Peter Halldin, PhD Karin Brolin, PhD Magnus Aare, MSc Sofia Hedenstierna and MSc Daniel Lanner.

The contractor has since the project start sent 9 interim reports:

- N62558-03-C-0013_Interim_1.pdf
- N62558-03-C-0013_Interim_2.pdf
- N62558-03-C-0013_Interim_3_040708.pdf
- N62558-03-C-0013_Interim_5_041215.pdf
- N62558-03-C-0013_Interim_6_050331.pdf
- N62558-03-C-0013_Interim_7_050631.pdf
- N62558-03-C-0013_Interim_9_051227.pdf
- N62558-03-C-0013_Interim_10_060331.pdf
- N62558-03-C-0013_Interim_11_060630.pdf

and 3 final reports according to the contract *No: N62558-03-C-0013*.

- N62558-03-C-0013_Phase1_040931.pdf
- N62558-03-C-0013_Final_Phase2_050930-3.pdf
- N62558-03-C-0013_Final_Phase3_060930.pdf (this report)

The contractor has delivered all result files generated by the KTH neck model simulations to Titan Corporation (L3 Communications) in San Diego. The results have then been prepared and included in a web based Graphical User Interface (GUI), by Titan Corporation. The result files include:

- animation files (d3plot),
- normalized ligament deformation (deforce),
- vertebral stress and disc pressure (elout) and
- forces and moments for the lower neck (jntforc)

The contractor has also delivered:

- a post-processor built in Matlab that is used to calculate the normalized ligament deformation, beam criteria and von Mises stress values, Figure 35.
- Movies from the simulations (mpeg).

The contractor has during this three year project participated in:

- six project meetings in US,
- an experimental EMG study on muscle activation in human subjects during voluntary and sled perturbations conducted by G Siegmund and J-S Blouin at MEA in Vancouver, BC.

And presented results from the project at:

- the ASMA annual conference 18th of May in Orlando. Halldin P, Brolin K, Hedenstierna S. *Finite element analysis of helicopter pilot neck injuries.*
- The ICrash 2006 Conference, Greece. Brolin K, Hedenstierna, Halldin P, Alem N. *The importance of muscle tension on the outcome of impacts with a major vertical component.*
- the World Congress of Biomechanics 4th of August in Munich. Halldin P, Brolin K, Hedenstierna S, Lanner D and Alem N. *FE modelling of the neck responses in 3D loading and the influence of muscle activation for HSM evaluations.*

The contractor has sent three scientific papers for publication.

- Hedenstierna S. Brolin K, Halldin P, Alem N, *FE-simulation of Mechanical Testing of a Rabbit Tibialis Anterior Muscle.* Submitted to Aviation, Space, and Environmental Medicine
- Halldin P, Brolin K, Aare M, Hedenstierna S. Alem N. *Analysis of head supported mass and the risk for neck injuries at rear end, vertical, frontal, lateral and oblique impacts* – A numerical analysis. Submitted to Aviation, Space, and Environmental Medicine.
- Brolin K, Halldin P, Hedenstierna S. Alem N. *The importance of muscle tension on the outcome of impacts with a major vertical component.* Submitted to the International Journal of Crashworthiness.

The contractor has also sent two technical reports to USAARL.

- Aare M, Halldin P, Brolin K. *Validation of the KTH neck model using cadaver component tests.* Technical Report. KTH School of Technology and Health, The Royal Institute of Technology. August 2005.

- Hedenstierna S, *The KTH visit to the EMG study on muscle activation in human subjects during voluntary and sled pertubations* conducted by G Siegmund and J-S Blouin at MEA in Vancouver, BC. Technical Report. KTH School of Technology and Health, The Royal Institute of Technology. March 2005.

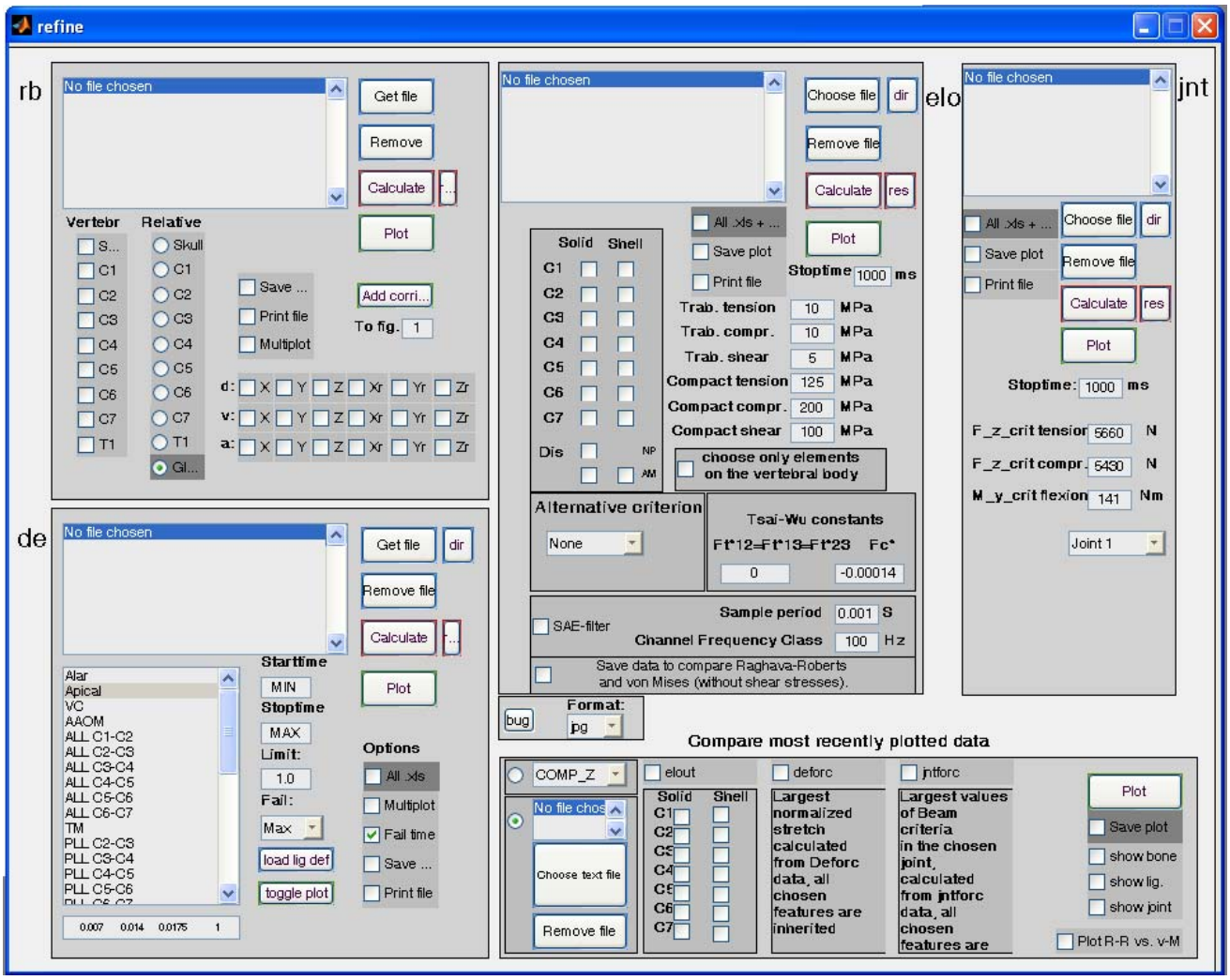

Figure 35. Image of the postprocessor used to handle the large output files from the simulations.

7 Acknowledgements

Axel Nordberg and Daniel Lanner are acknowledged for their programming efforts with the Matlab post-processor.

Kofi Amankwah is acknowledge for his help and support with implementing the results from the KTH neck model in the GUI.

Dr Dale Bass and the UVA staff are acknowledge for there support with experimental data used to validate the KTH neck model in the Oblique XZ impacts.

Dr Nabih Alem and Dr Carol Chancey are acknowledged for their positive and constructive leader chip in the HSM project.

8 References

Anderson J., Hsu A., Vasavada A. Morphology, Architecture, and Biomechanics of Human Cervical Multifidus. Spine, Vol 30, Nr 4, pp E86-E91, 2005.

Ashrafiuon H, Alem NM and McEntire. Effects of Weight and Center of Gravity Location of Head-Supported Devices on Neck Loading. Aviation, Space and Environmental Medicine, 68 (10), 915-922, 1997.

Bass C R, Salzar R, Donnellan L and Lucas S. Injury Risk From HSM Loading (HM2,3,4,5 Series). University of Virginia, Center for Applied Biomechanics, Nov 2004, Report HEADMASS2, 2004.

Benfer R. Morphometric Analysis of Cartesian Coordinates of the Human Skull. Am J. phys. Anthrop, 42: pp 371-382, 1975.

Best T.M. A Biomechanical Study of Skeletal Muscle Strain Injuries. Dissertation. Department of Biomedical Engineering, Duke University, 1993

Brolin K (2002) Cervical Spinal Injuries – Numerical Analyses and Statistical Survey, Doctoral Thesis, Department of Aeronautics, KTH, Report 2002-29, Stockholm, Sweden.

Brolin K, Halldin P, Leijonhufvud I. (2005) The Effect of Muscle Activation on Neck Response. Traffic Injury Prevention, Vol 6, Issue 1, pp. 67-76.

Chancey C., Nightingale R., Van Ee C., Knaub K., Myers B. Improved Estimation of Human Neck Tensile Tolerance: Reducing the Range of Reported Tolerance Using Anthropometrically Correct Muscles and Optimized Physiologic Initial Conditions. Proceedings of the 47th Stapp Car Crash Conference 2003, pages 135-153.

Currey JD. Tensile yield in compact bone is determined by strain, post-yield behaviour by mineral content. J. of Biomechanics. Vol 37, pages 549-556. 2004.

Coakwell MR, Bloswick DS, Moser R. High-Risk Head and Neck Movements at High G and Interventions to Reduce Associated Neck Injury. Aviation, Space and Environmental Medicine, 75 (1), 68-80, 2004.

Davidsson Johan, Development of a Mechanical Model for Rear Impacts. Doctoral Thesis, Chalmers Technical University, Gothenburg, Sweden. 2000.

Ewing CL, Thomas DJ, Lustick L, Muzzy III WH, Williams G, Majewski PL, The Effect of Duration, Rate of Onset and Peak Sled Acceleration on the Dynamic Response of the Human Head and Neck, Proceedings of the 20th Stapp Car Crash Conference, 1976

Ewing CL, Thomas DJ, Lustick L, Muzzy III WH, Williams GC, Majewski P, Effect of Initial Position on the Human Head and Neck Response to +Y Impact Acceleration, Proceedings of the 20th Stapp Car Crash Conference, 1976

Goel V., Liu K., Clark C. Quantitative Geometry of the Muscular Origins and Insertions of the Human Head and Neck. Mechanisms of Head and Spine Trauma, Aloray Publisher, editor

Sances Jr. A., Thomas, D.J., Ewing, C.L., Larson, S.J., and Unterharnscheidt, F., pp:397-415, Goshen, New York, 1986

Green N D C, Acute Soft Tissue Neck Injury from Unexpected Acceleration. Aviation, Space, and Envionmental Medicine, 74 (10), 2003.

Halldin PH, Lotta Jakobsson, Karin Brolin, Camilla Palmertz, Svein Kleiven and Hans von Holst. Investigation of Conditions that Affect Neck Compression-Flexion Injuries Using Numerical Techniques. the 44th STAPP Car Crash Journal, 2000-01-SC10 2000).

Halldin P, Brolin K, von Holst, H. Hedenstierna S, Aare M. Finite element analysis of the effects of head-supported mass on neck responses. (2004) Complete Phase One Report, Contract NO: N62558-03-C-0013, UNITED STATES ARMY EUROPEAN RESEARCH OFFICE OF THE U.S. ARMY, London, England September 2004.

Halldin P, Brolin K, Hedenstierna S, Aare M, von Holst, H. Finite element analysis of the effects of head-supported mass on neck responses. (2005) Complete Phase Two Report, Contract NO: N62558-03-C-0013, UNITED STATES ARMY EUROPEAN RESEARCH OFFICE OF THE U.S. ARMY, London, England September 2005

Hallquist JO. (1998) LS-DYNA Theoretical Manual, Livermoore Software Technology Corporation. 1998.

Hawkins D., Bey M. Muscle and Tendon Force-Length Properties and their Interactions in vivo. J.Biomechanics, vol 30, nr1, pp 63-70, 1997

Iida et al. The Spine Journal. 2 (2002) 95-100.

Johansson T., Meier P., Blickhan R. A Finite-Element Model for the Mechanical Analysis of Skeletal Muscles. Journal of theoretical biology, 206, pp 131-149, 2000

Kamibayashi L., Richmond F. Morphometry of Human Neck Muscles. Spine, 23, pp1314-1323, 1998.

Kleiven (2002), Finite Element Modeling of the Human Head. Doctoral Thesis. Report 2002-9, Institutionen för flygteknik, Kungliga tekniska högskolan, Stockholm, Sverige. 2002.

Kramer M., Schmidt I., Snader S., Högel J., Eisele R., Kinzl L., Hartwig E. Guidelines for the intramuscular positioning of EMG electrodes in the semispinalis Capitis and Cervicis muscles. Journal of Electromyography and Kinesiology 13 pp 289-295, 2003

Manoogian S, Kennedy E, Wilson K, Duma S. Injury Criteria and Parametric Analysis of Musculoskeletal Injuries to the Human Neck Due to Added Head-Supported Mass. Final Report. Center for Injury Mechanics, Virginia, Report Number 2005-080, 2005.

Mayoux-Benhamou MA., Barbet JP., Bargy F., Vallée C., Revel M. Method of quantitative anatomical study of the dorsal neck muscles. Surg Radiol Anat. 12 pp 181 - 185, 1990

Myers B., Van Ee C., Camacho DLA., Woolley CT., Best TM. On the Structural and Mateiral Properties of Mammalian Skeletal Muscle and Its Relevance to Human Cervical Impact Dynamics. Proceedings of the 39th Stapp Car Crash Conference 1995

Myers B., Woolley C.T., Slotter T.L., Garrett W.E., Best T.M. The Influence of Strain Rate on the Passive and Stimulated Engineering Stress-Large Strain Behavior of the Rabbit Tibialis Anterior Muscle. J. Biomechanical Engineering, 120(1), pp 126-132, 1998

Myklebust JB, Pintar F, Yoganandan N, Cusick JF, Maiman D, Myers TJ, Sances A. (1988) Tensile strength of spinal ligaments, SPINE, 13: (5) 526-531

NIST/SEMATECH e-Handbook of Statistical Methods , http://www.itl.nist.gov/div898/handbook/, 2006.

Ogden R.W. Large Deformation Isotropic Elasticity:On the Correlation of Theory and Experiment for Copmressible Rubberlike Solids. Proc. R.Soc. Lond. A. 38, 567-583, 1972

Panjabi M.M., Ito S., Pearson A.M. and Ivancic P.C., 2004, Injury Mechanism of the Cervical Intervertebral Disc During Simulated Whiplash, Spine, Vol. 29, Nr. 11, pp 1217-1225, 2004.

Shanahan DF and Shanahan MO. Injury in US Army helicopter crashes fiscal years October 1979 – September 1985. Journal of Trauma. 29(4):415-423; 1989

Shannon SG and Mason KT. US Army Aviation Life Support Equipment Retrieval Program. Head and Neck Injury Among Night Vision Goggle Users in Rotary-Wing Mishaps. USAARL Report Nr. 98-02, 1997.

Yamada H (1973). Strength of Biological Materials. Evans F G (Ed), Huntington. N.Y.

Yoganandan N, Pintar F, Butler J, Reinartz J, Sances A, Larson SJ. (1989) Dynamic Resonse of Human Cervical Spine Ligaments, SPINE, 14: (10) 1102-1109

van der Horst M Human Head Neck Response in Frontal, Lateral and Rear End Impact Loading. Dissertation: Eindhoven Technische Universiteit, 2002

Vasavada A., Li S., Delp S. Influence of Muscle Morphometry and Moment Arms on the Moment-Generating Capacity of Human Neck Muscles. Spine, Vol 23, Nr 4, pp 412-422, 1998

Winters JM., Stark L. Estimated mechanical properties of synergistic muscles involved in movements of a variety of human joints. Journal of Biomechanics, Vol. 21, pp. 1027-41, 1988

Wittek A. Mathematical Modeling of the Muscle Effects on the Human Body Responses under Transient Loads. Dissertation, Department of the Human Factors Engineering, Chalmers University of Technology 2000.

Appendix A - New simulation results

A1 – Vertical impact resulting in a compression of the neck.

Results COMP_Z	Beam Criteria	Normalized ligament deformation		Normalized stress in bone			
				Trabecular		Compact	
Relaxed activation	BC without Fx	Norm def.	Ligament	C3	C5	C3	C5
COMP Z 13,5G 0kg	0,27	0,73	ISL C4-C5	0,25	0,30	0,28	0,16
COMP Z 13,5G 1kg X2 Z2cm	0,35	0,74	ISL C4-C5	0,31	0,33	0,34	0,17
COMP Z 13,5G 2kg X2 Z2cm	0,42	0,79	ISL C4-C5	0,35	0,32	0,38	0,20
COMP Z 13,5G 2kg X-2 Z2cm	0,48	0,66	ISL C4-C5	0,36	0,28	0,36	0,22
COMP Z 13,5G 2kg X2 Z-2cm	0,41	0,81	ISL C4-C5	0,35	0,43	0,38	0,22
COMP Z 13,5G 2kg X2 Z6cm	0,44	0,76	ISL C4-C5	0,35	0,30	0,38	0,20
COMP Z 13,5G 2kg X6 Z2cm	0,41	0,90	ISL C6-C7	0,35	0,48	0,36	0,25
COMP Z 13,5G 3kg X2 Z2cm	0,51	0,81	ISL C4-C5	0,41	0,34	0,41	0,22
COMP Z 22G 0kg	0,49	0,86	ISL C4-C5	0,39	0,50	0,40	0,25
COMP Z 22G 1kg X-2 Z-2cm	0,63	0,85	ISL C6-C7	0,50	0,40	0,38	0,25
COMP Z 22G 1kg X-2 Z6cm	0,71	0,87	ISL C6-C7	0,49	0,37	0,38	0,25
COMP Z 22G 1kg X6 Z-2cm	0,72	0,98	ISL C6-C7	0,45	0,56	0,43	0,28
COMP Z 22G 1kg X6 Z6cm	0,65	0,97	ISL C6-C7	0,46	0,49	0,42	0,26
COMP Z 22G 2kg X2 Z2cm	0,74	0,94	ISL C6-C7	0,57	0,53	0,42	0,27
COMP Z 22G 3kg X-2 Z-2cm	0,93	1,29	ISL C6-C7	0,62	0,38	0,43	0,32
COMP Z 22G 3kg X-2 Z6cm	0,95	1,32	ISL C6-C7	0,64	0,41	0,39	0,33
COMP Z 22G 3kg X6 Z-2cm	0,87	1,10	ISL C6-C7	0,67	0,70	0,47	0,31
COMP Z 22G 3kg X6 Z6cm	0,81	0,91	ISL C4-C5	0,67	0,50	0,53	0,25
COMP Z 5G 0kg	0,10	0,31	ISL C3-C4	0,12	0,12	0,13	0,07
COMP Z 5G 1kg X-2 Z-2cm	0,13	0,28	ISL C3-C4	0,14	0,12	0,16	0,08
COMP Z 5G 1kg X-2 Z6cm	0,13	0,31	ISL C3-C4	0,14	0,12	0,16	0,09
COMP Z 5G 1kg X6 Z-2cm	0,12	0,41	ISL C4-C5	0,14	0,17	0,16	0,09
COMP Z 5G 1kg X6 Z6cm	0,13	0,44	ISL C3-C4	0,15	0,17	0,16	0,09
COMP Z 5G 2kg X2 Z2cm	0,16	0,47	ISL C4-C5	0,17	0,18	0,19	0,10
COMP Z 5G 3kg X-2 Z-2cm	0,19	0,35	ISL C4-C5	0,19	0,15	0,22	0,12
COMP Z 5G 3kg X-2 Z6cm	0,20	0,29	ISL C3-C4	0,18	0,14	0,22	0,13
COMP Z 5G 3kg X6 Z-2cm	0,18	0,60	ISL C4-C5	0,21	0,27	0,20	0,15
COMP Z 5G 3kg X6 Z6cm	0,17	0,61	ISL C4-C5	0,21	0,26	0,20	0,15
Tensed activation							
COMP Z 13G 2kg X2 Z2cm	0,56	0,58	ISL C6-C7	0,50	0,36	0,39	0,29
COMP Z 22G 2kg X2 Z2cm	0,76	0,92	ISL C6-C7	0,62	0,45	0,47	0,31
COMP Z 5G 2kg X2 Z2cm	0,48	0,30	ISL C4-C5	0,45	0,34	0,35	0,27

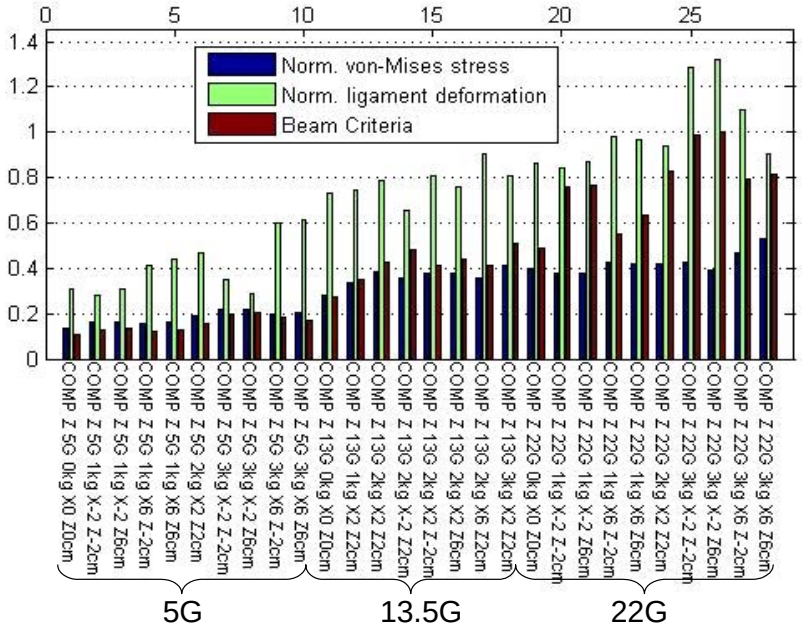

A2 – Frontal impact resulting in a flexion bending of the neck.

Results FLEX_X	Beam Criteria	Normalized ligament deformation		Normalized stress in bone			
				Trabecular		Compact	
Relaxed activation		Norm def.	Ligament	C3	C5	C3	C5
FLEX X 13G 0kg	0,68	1,24	ISL C6-C7	0,52	0,69	0,35	0,35
FLEX X 13,5G 1kg X2 Z2cm	0,74	1,27	ISL C6-C7	0,59	0,74	0,41	0,37
FLEX X 13,5G 2kg X2 Z2cm	0,79	1,32	ISL C6-C7	0,63	0,75	0,40	0,38
FLEX X 13,5G 2kg X-2 Z2cm	0,81	1,31	ISL C6-C7	0,65	0,68	0,36	0,38
FLEX X 13,5G 2kg X2 Z-2cm	0,75	1,32	ISL C6-C7	0,59	0,80	0,43	0,38
FLEX X 13,5G 2kg X2 Z6cm	0,83	1,34	ISL C6-C7	0,67	0,69	0,36	0,39
FLEX X 13,5G 2kg X6 Z2cm	0,77	1,33	ISL C6-C7	0,62	0,71	0,36	0,38
FLEX X 13,5G 3kg X2 Z2cm	0,83	1,38	ISL C6-C7	0,67	0,75	0,40	0,40
FLEX X 22G 0kg	0,93	1,60	ISL C6-C7	0,77	0,83	0,48	0,46
FLEX X 22G 1kg X-2 Z-2cm	0,99	1,66	ISL C6-C7	0,81	0,88	0,49	0,47
FLEX X 22G 1kg X-2 Z6cm	1,02	1,67	ISL C6-C7	0,88	0,93	0,52	0,48
FLEX X 22G 1kg X6 Z-2cm	1,00	1,66	ISL C6-C7	0,77	0,79	0,43	0,47
FLEX X 22G 1kg X6 Z6cm	1,02	1,68	ISL C6-C7	0,82	0,87	0,47	0,48
FLEX X 22G 2kg X2 Z2cm	1,08	1,74	ISL C6-C7	0,88	0,93	0,53	0,50
FLEX X 22G 3kg X-2 Z-2cm	1,20	1,83	ISL C6-C7	0,89	0,93	0,53	0,52
FLEX X 22G 3kg X-2 Z6cm	1,13	1,80	ISL C6-C7	0,99	1,04	0,64	0,53
FLEX X 22G 3kg X6 Z-2cm	1,15	1,78	ISL C6-C7	0,81	0,85	0,51	0,51
FLEX X 22G 3kg X6 Z6cm	1,19	1,84	ISL C6-C7	0,92	0,97	0,58	0,54
FLEX X 5G 0kg	0,26	0,76	ISL C4-C5	0,26	0,34	0,18	0,18
FLEX X 5G 1kg X-2 Z-2cm	0,28	0,75	ISL C4-C5	0,27	0,36	0,19	0,19
FLEX X 5G 1kg X-2 Z6cm	0,31	0,76	ISL C4-C5	0,27	0,34	0,19	0,18
FLEX X 5G 1kg X6 Z-2cm	0,28	0,76	ISL C4-C5	0,25	0,32	0,18	0,17
FLEX X 5G 1kg X6 Z6cm	0,31	0,77	ISL C4-C5	0,25	0,32	0,19	0,17
FLEX X 5G 2kg X2 Z2cm	0,34	0,78	ISL C4-C5	0,30	0,37	0,20	0,19
FLEX X 5G 3kg X-2 Z-2cm	0,32	0,77	ISL C4-C5	0,27	0,35	0,21	0,19
FLEX X 5G 3kg X-2 Z6cm	0,41	0,81	ISL C2-C3	0,33	0,41	0,24	0,20
FLEX X 5G 3kg X6 Z-2cm	0,31	0,75	ISL C4-C5	0,28	0,36	0,23	0,20
FLEX X 5G 3kg X6 Z6cm	0,40	0,81	ISL C4-C5	0,32	0,42	0,26	0,21
Tensed activation							
FLEX X 13G 2kg X2 Z2cm	0,69	1,34	ISL C6-C7	0,52	0,71	0,47	0,43
FLEX X 22G 2kg X2 Z2cm	0,95	1,69	ISL C6-C7	0,69	1,01	0,55	0,69
FLEX X 5G 2kg X2 Z2cm	0,54	0,84	ISL C4-C5	0,51	0,39	0,39	0,28

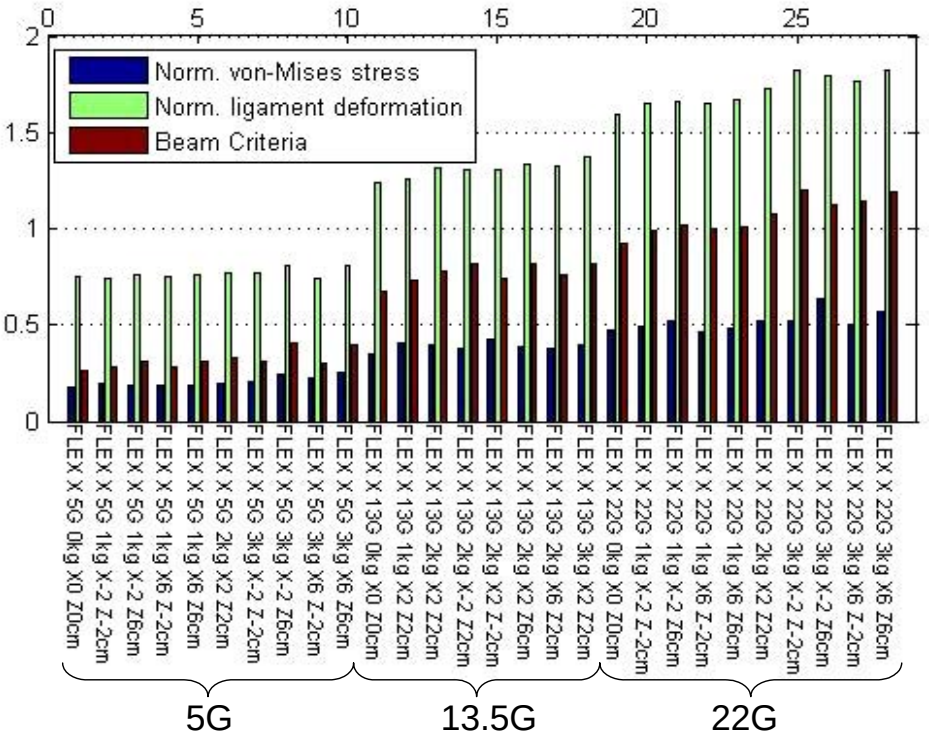

A3 – Sagittal plane oblique impact resulting in a compression/flexion of the neck.

Results OBL_XZ	Beam Criteria	Normalized ligament deformation		Normalized stress in bone			
				Trabecular		Compact	
Relaxed activation		Norm def.	Ligament	C3	C5	C3	C5
OBL_XZ_13G_0kg_X0_Z0cm	0,67	1,24	ISL C6-C7	0,51	0,70	0,37	0,35
OBL_XZ_13G_1kg_X2_Z2cm	0,73	1,26	ISL C6-C7	0,58	0,71	0,38	0,36
OBL_XZ_13G_2kg_X2_Z2cm	0,78	1,33	ISL C6-C7	0,63	0,74	0,39	0,39
OBL_XZ_13G_2kg_X-2_Z2cm	0,74	1,21	ISL C6-C7	0,60	0,65	0,37	0,35
OBL_XZ_13G_2kg_X2_Z-2cm	0,77	1,38	ISL C6-C7	0,62	0,86	0,44	0,40
OBL_XZ_13G_2kg_X2_Z6cm	0,79	1,30	ISL C6-C7	0,64	0,69	0,37	0,38
OBL_XZ_13G_2kg_X6_Z2cm	0,81	1,43	ISL C6-C7	0,66	0,79	0,42	0,42
OBL_XZ_13G_3kg_X2_Z2cm	0,81	1,38	ISL C6-C7	0,66	0,75	0,39	0,41
OBL_XZ_22G_0kg_X0_Z0cm	1,10	1,73	ISL C6-C7	0,85	0,90	0,49	0,51
OBL_XZ_22G_1kg_X-2_Z-2cm	1,14	1,78	ISL C6-C7	0,87	0,92	0,52	0,52
OBL_XZ_22G_1kg_X-2_Z6cm	1,03	1,69	ISL C6-C7	0,90	0,93	0,54	0,50
OBL_XZ_22G_1kg_X6_Z-2cm	1,33	1,93	ISL C6-C7	0,89	0,95	0,54	0,58
OBL_XZ_22G_1kg_X6_Z6cm	1,20	1,85	ISL C6-C7	0,92	0,96	0,57	0,55
OBL_XZ_22G_2kg_X2_Z2cm	1,27	1,90	ISL C6-C7	0,98	1,00	0,61	0,57
OBL_XZ_22G_3kg_X-2_Z-2cm	1,38	1,99	ISL C6-C7	0,95	0,98	0,61	0,60
OBL_XZ_22G_3kg_X-2_Z6cm	1,10	1,77	ISL C6-C7	0,97	1,02	0,63	0,53
OBL_XZ_22G_3kg_X6_Z-2cm	1,71	2,24	ISL C6-C7	0,96	1,04	0,60	0,70
OBL_XZ_22G_3kg_X6_Z6cm	1,45	2,04	ISL C6-C7	1,02	1,06	0,68	0,60
OBL_XZ_5G_0kg_X0_Z0cm	0,21	0,68	ISL C4-C5	0,22	0,30	0,17	0,16
OBL_XZ_5G_1kg_X-2_Z-2cm	0,21	0,68	ISL C4-C5	0,23	0,30	0,18	0,16
OBL_XZ_5G_1kg_X-2_Z6cm	0,22	0,69	ISL C4-C5	0,21	0,27	0,16	0,15
OBL_XZ_5G_1kg_X6_Z-2cm	0,23	0,72	ISL C4-C5	0,26	0,34	0,20	0,18
OBL_XZ_5G_1kg_X6_Z6cm	0,24	0,71	ISL C4-C5	0,22	0,29	0,17	0,15
OBL_XZ_5G_2kg_X2_Z2cm	0,27	0,73	ISL C4-C5	0,24	0,31	0,19	0,17
OBL_XZ_5G_3kg_X-2_Z-2cm	0,24	0,70	ISL C4-C5	0,24	0,33	0,19	0,17
OBL_XZ_5G_3kg_X-2_Z6cm	0,30	0,74	ISL C4-C5	0,27	0,34	0,21	0,17
OBL_XZ_5G_3kg_X6_Z-2cm	0,31	0,79	ISL C4-C5	0,29	0,37	0,23	0,20
OBL_XZ_5G_3kg_X6_Z6cm	0,34	0,78	ISL C4-C5	0,30	0,39	0,24	0,20
Tensed activation							
OBL_XZ_13G_2kg_X2_Z2cm	0,61	1,11	ISL C4-C5	0,52	0,71	0,40	0,41
OBL_XZ_22G_2kg_X2_Z2cm	0,91	1,79	ISL C4-C5	0,73	1,15	0,51	0,70
OBL_XZ_5G_2kg_X2_Z2cm	0,52	0,88	ISL C4-C5	0,48	0,35	0,36	0,28

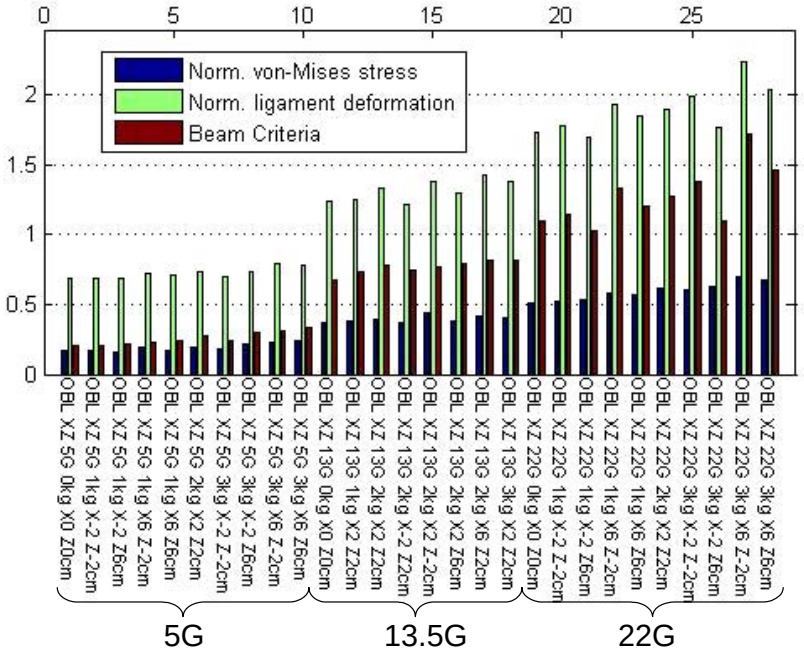

KTH VETENSKAP OCH KONST

KTH Technology and Health

A4 – Lateral impact resulting in lateral bending of the neck.

Results LAT_Y	**Beam Criteria**	**Normalized ligament deformation**		**Normalized stress in bone**			
				Trabecular		Compact	
Relaxed activation		30 year		C3	C5	C3	C5
LAT Y 13G 0kg X0 Z0cm	-	0,83	PLL C5-C6	0,60	0,75	0,38	0,48
LAT Y 13G 1kg X2 Z2cm	-	0,88	PLL C5-C6	0,64	0,79	0,41	0,52
LAT Y 13G 2kg X2 Z2cm	-	0,95	PLL C5-C6	0,68	0,85	0,44	0,55
LAT Y 13G 2kg X-2 Z2cm	-	0,93	PLL C5-C6	0,69	0,83	0,45	0,54
LAT Y 13G 2kg X2 Z-2cm	-	0,91	PLL C5-C6	0,62	0,80	0,40	0,53
LAT Y 13G 2kg X2 Z6cm	-	0,97	PLL C5-C6	0,70	0,86	0,46	0,56
LAT Y 13G 2kg X6 Z2cm	-	0,94	PLL C5-C6	0,67	0,86	0,44	0,56
LAT Y 13G 3kg X2 Z2cm	-	0,92	TM	0,66	0,82	0,43	0,54
LAT Y 22G 0kg X0 Z0cm	-	1,25	PLL C5-C6	0,82	1,04	0,57	0,67
LAT Y 22G 1kg X-2 Z-2cm	-	1,37	PLL C5-C6	0,83	1,07	0,61	0,70
LAT Y 22G 1kg X-2 Z6cm	-	1,41	PLL C5-C6	0,86	1,09	0,65	0,72
LAT Y 22G 1kg X6 Z-2cm	-	1,38	PLL C5-C6	0,82	1,10	0,60	0,72
LAT Y 22G 1kg X6 Z6cm	-	1,44	PLL C5-C6	0,88	1,12	0,66	0,75
LAT Y 22G 2kg X2 Z2cm	-	1,55	PLL C5-C6	0,89	1,17	0,69	0,78
LAT Y 22G 3kg X-2 Z-2cm	-	1,70	PLL C5-C6	0,65	0,82	0,43	0,58
LAT Y 22G 3kg X-2 Z6cm	-	1,76	PLL C5-C6	1,03	1,19	0,79	0,84
LAT Y 22G 3kg X6 Z-2cm	-	1,68	PLL C5-C6	0,88	1,19	0,67	0,81
LAT Y 22G 3kg X6 Z6cm	-	1,76	PLL C4-C5	0,97	1,23	0,75	0,87
LAT Y 5G 0kg X0 Z0cm	-	0,50	CL C1-C2	0,25	0,27	0,23	0,21
LAT Y 5G 1kg X-2 Z-2cm	-	0,53	CL C1-C2	0,23	0,27	0,21	0,21
LAT Y 5G 1kg X-2 Z6cm	-	0,59	CL C1-C2	0,25	0,31	0,22	0,22
LAT Y 5G 1kg X6 Z-2cm	-	0,52	CL C1-C2	0,23	0,28	0,22	0,20
LAT Y 5G 1kg X6 Z6cm	-	0,59	CL C1-C2	0,25	0,31	0,22	0,21
LAT Y 5G 2kg X2 Z2cm	-	0,61	CL C1-C2	0,26	0,32	0,22	0,22
LAT Y 5G 3kg X-2 Z-2cm	-	0,56	CL C1-C2	0,24	0,28	0,22	0,22
LAT Y 5G 3kg X-2 Z6cm	-	0,75	CL C1-C2	0,30	0,36	0,23	0,22
LAT Y 5G 3kg X6 Z-2cm	-	0,59	CL C1-C2	0,24	0,32	0,20	0,21
LAT Y 5G 3kg X6 Z6cm	-	0,72	CL C1-C2	0,29	0,36	0,22	0,21
Tensed activation							
LAT Y 13G 2kg X2 Z2cm	-	0,79	PLL C5-C6	0,60	0,64	1,00	0,43
LAT Y 22G 2kg X2 Z2cm	-	1,37	PLL C5-C6	0,84	0,98	1,06	0,53
LAT Y 5G 2kg X2 Z2cm	-	0,37	CL C1-C2	0,47	0,37	0,69	0,38

KTH VETENSKAP OCH KONST

KTH Technology and Health

A5 – Horizontal plane oblique impact impact resulting in a flexion/lateral bending of the neck.

Results OBL_XY	Beam Criteria	Normalized ligament deformation		Normalized stress in bone			
				Trabecular		Compact	
Relaxed activation		Norm def.	Ligament	C3	C5	C3	C5
OBL XY 13G 0kg	-	0,92	ISL C6-C7	0,56	0,70	0,40	0,42
OBL XY 13G 1kg X2 Z2cm	-	0,97	ISL C6-C7	0,62	0,73	0,38	0,42
OBL XY 13G 2kg X2 Z2cm	-	1,02	ISL C6-C7	0,66	0,73	0,40	0,44
OBL XY 13G 2kg X-2 Z2cm	-	1,02	ISL C6-C7	0,69	0,74	0,41	0,44
OBL XY 13G 2kg X2 Z-2cm	-	1,01	ISL C6-C7	0,57	0,65	0,33	0,42
OBL XY 13G 2kg X2 Z6cm	-	1,06	ISL C6-C7	0,64	0,72	0,40	0,44
OBL XY 13G 2kg X6 Z2cm	-	1,02	ISL C6-C7	0,63	0,72	0,38	0,44
OBL XY 13G 3kg X2 Z2cm	-	1,09	ISL C6-C7	0,71	0,78	0,43	0,46
OBL XY 22G 0kg	-	1,27	ISL C6-C7	0,80	0,91	0,53	0,54
OBL XY 22G 1kg X-2 Z-2cm	-	1,34	ISL C6-C7	0,83	0,99	0,59	0,53
OBL XY 22G 1kg X-2 Z6cm	-	1,41	ISL C6-C7	0,86	0,97	0,61	0,57
OBL XY 22G 1kg X6 Z-2cm	-	1,33	ISL C6-C7	0,82	0,95	0,56	0,57
OBL XY 22G 1kg X6 Z6cm	-	1,35	ISL C6-C7	0,84	0,96	0,58	0,56
OBL XY 22G 2kg X2 Z2cm	-	1,42	ISL C6-C7	0,89	1,02	0,66	0,59
OBL XY 22G 3kg X-2 Z-2cm	-	1,47	ISL C6-C7	0,85	1,00	0,61	0,58
OBL XY 22G 3kg X-2 Z6cm	-	1,60	ISL C6-C7	0,98	1,04	0,72	0,64
OBL XY 22G 3kg X6 Z-2cm	-	1,44	ISL C6-C7	0,82	1,00	0,56	0,62
OBL XY 22G 3kg X6 Z6cm	-	1,56	ISL C6-C7	0,91	1,05	0,69	0,61
OBL XY 5G 0kg	-	0,58	ISL C4-C5	0,26	0,29	0,14	0,21
OBL XY 5G 1kg X-2 Z-2cm	-	0,57	ISL C4-C5	0,25	0,28	0,14	0,21
OBL XY 5G 1kg X-2 Z6cm	-	0,59	ISL C4-C5	0,26	0,28	0,15	0,20
OBL XY 5G 1kg X6 Z-2cm	-	0,56	ISL C4-C5	0,26	0,28	0,15	0,20
OBL XY 5G 1kg X6 Z6cm	-	0,59	ISL C4-C5	0,27	0,29	0,15	0,21
OBL XY 5G 2kg X2 Z2cm	-	0,59	ISL C3-C4	0,30	0,30	0,16	0,21
OBL XY 5G 3kg X-2 Z-2cm	-	0,60	ISL C4-C5	0,29	0,31	0,16	0,22
OBL XY 5G 3kg X-2 Z6cm	-	0,68	ISL C2-C3	0,32	0,35	0,17	0,22
OBL XY 5G 3kg X6 Z-2cm	-	0,58	ISL C4-C5	0,28	0,31	0,19	0,20
OBL XY 5G 3kg X6 Z6cm	-	0,62	ISL C4-C5	0,29	0,33	0,16	0,22
Tensed activation							
OBL XY 13G 2kg X2 Z2cm	-	0,86	LF C6-C7	0,66	0,65	0,54	0,50
OBL XY 22G 2kg X2 Z2cm	-	1,29	ISL C6-C7	0,79	0,86	0,61	0,59
OBL XY 5G 2kg X2 Z2cm	-	0,70	ISL C3-C4	0,48	0,36	0,41	0,30

KTH VETENSKAP OCH KONST

KTH Technology and Health

A6 – Frontal plane oblique impact resulting in a compression/lateral bending of the neck.

Results OBL_YZ	Beam Criteria	Normalized ligament deformation		Normalized stress in bone			
				Trabecular		Compact	
Relaxed activation		Norm def.	Ligament	C3	C5	C3	C5
OBL YZ 13G 0kg		0,72	PLL C5-C6	0,53	0,65	0,33	0,39
OBL YZ 13G 1kg X2 Z2cm		0,76	CL C1-C2	0,55	0,67	0,35	0,40
OBL YZ 13G 2kg X2 Z2cm		0,81	CL C1-C2	0,57	0,70	0,37	0,42
OBL YZ 13G 2kg X-2 Z2cm		0,81	CL C1-C2	0,56	0,67	0,37	0,42
OBL YZ 13G 2kg X2 Z-2cm		0,79	PLL C5-C6	0,57	0,70	0,36	0,42
OBL YZ 13G 2kg X2 Z6cm		0,89	CL C1-C2	0,58	0,71	0,39	0,43
OBL YZ 13G 2kg X6 Z2cm		0,82	CL C1-C2	0,60	0,74	0,38	0,43
OBL YZ 13G 3kg X2 Z2cm		0,84	CL C1-C2	0,60	0,73	0,39	0,44
OBL YZ 22G 0kg		1,10	PLL C5-C6	0,78	0,96	0,52	0,59
OBL YZ 22G 1kg X-2 Z-2cm		1,22	PLL C5-C6	0,79	0,97	0,56	0,61
OBL YZ 22G 1kg X-2 Z6cm		1,22	PLL C5-C6	0,80	1,02	0,61	0,64
OBL YZ 22G 1kg X6 Z-2cm		1,21	PLL C5-C6	0,82	1,01	0,55	0,62
OBL YZ 22G 1kg X6 Z6cm		1,24	PLL C5-C6	0,83	1,05	0,60	0,64
OBL YZ 22G 2kg X2 Z2cm		1,36	PLL C5-C6	0,87	1,07	0,63	0,65
OBL YZ 22G 3kg X-2 Z-2cm		1,50	ISL C5-C6	0,87	0,98	0,61	0,68
OBL YZ 22G 3kg X-2 Z6cm		1,58	PLL C5-C6	0,86	0,99	0,67	0,73
OBL YZ 22G 3kg X6 Z-2cm		1,41	PLL C5-C6	0,89	1,14	0,65	0,68
OBL YZ 22G 3kg X6 Z6cm		1,93	CL C1-C2	0,94	1,15	0,73	0,72
OBL YZ 5G 0kg		0,41	CL C1-C2	0,21	0,25	0,19	0,17
OBL YZ 5G 1kg X-2 Z-2cm		0,44	CL C1-C2	0,23	0,26	0,22	0,19
OBL YZ 5G 1kg X-2 Z6cm		0,49	CL C1-C2	0,22	0,26	0,21	0,19
OBL YZ 5G 1kg X6 Z-2cm		0,44	CL C1-C2	0,23	0,23	0,20	0,16
OBL YZ 5G 1kg X6 Z6cm		0,47	CL C1-C2	0,22	0,24	0,20	0,18
OBL YZ 5G 2kg X2 Z2cm		0,52	CL C1-C2	0,25	0,24	0,21	0,17
OBL YZ 5G 3kg X-2 Z-2cm		0,51	CL C1-C2	0,29	0,25	0,23	0,18
OBL YZ 5G 3kg X-2 Z6cm		0,56	CL C1-C2	0,25	0,31	0,22	0,23
OBL YZ 5G 3kg X6 Z-2cm		0,52	CL C1-C2	0,28	0,26	0,17	0,19
OBL YZ 5G 3kg X6 Z6cm		0,52	CL C1-C2	0,24	0,29	0,21	0,21
Tensed activation							
OBL YZ 13G 2kg X2 Z2cm		0,74	CL C1-C2	0,49	0,51	1,09	0,41
OBL YZ 22G 2kg X2 Z2cm		1,17	PLL C5-C6	0,79	0,91	1,06	0,52
OBL YZ 5G 2kg X2 Z2cm		0,40	CL C1-C2	0,47	0,37	0,74	0,38

A7 – Rear end impact resulting in an extension of the neck.

Results EXT_-X File name	**Ligament** Norm fail value			**Normalized stress in bone** Trabecular		Compact	
	65 year	30 year		C3	C5	C3	C5
EXT_-X_3G_0kg_X0_Z0cm	1,14	0,91	ISL C4-C5	0,31	0,21	0,29	0,27
EXT_-X_3G_1kg_X-2_Z-2cm	1,14	0,91	ISL C4-C5	0,31	0,28	0,28	0,41
EXT_-X_3G_1kg_X-2_Z6cm	1,15	0,92	ISL C4-C5	0,32	0,31	0,28	0,38
EXT_-X_3G_1kg_X6_Z-2cm	1,14	0,91	ISL C4-C5	0,31	0,27	0,28	0,35
EXT_-X_3G_1kg_X6_Z6cm	1,15	0,92	ISL C4-C5	0,31	0,30	0,28	0,38
EXT_-X_3G_2kg_X2_Z2cm	1,13	0,90	ISL C4-C5	0,32	0,33	0,28	0,45
EXT_-X_3G_3kg_X-2_Z-2cm	1,15	0,92	ISL C4-C5	0,32	0,33	0,29	0,40
EXT_-X_3G_3kg_X-2_Z6cm	1,14	0,91	ISL C4-C5	0,33	0,35	0,28	0,42
EXT_-X_3G_3kg_X6_Z-2cm	1,13	0,90	ISL C4-C5	0,31	0,31	0,30	0,44
EXT_-X_3G_3kg_X6_Z6cm	1,14	0,91	ISL C4-C5	0,32	0,35	0,27	0,42
EXT_-X_5G_0kg_X0_Z0cm	1,15	0,92	ISL C4-C5	0,33	0,34	0,29	0,42
EXT_-X_5G_1kg_X-2_Z-2cm	1,18	0,95	ISL C4-C5	0,33	0,35	0,30	0,43
EXT_-X_5G_1kg_X-2_Z6cm	1,15	0,92	ISL C4-C5	0,33	0,36	0,29	0,44
EXT_-X_5G_1kg_X6_Z-2cm	1,16	0,93	ISL C4-C5	0,33	0,35	0,29	0,43
EXT_-X_5G_1kg_X6_Z6cm	1,14	0,91	ISL C4-C5	0,33	0,35	0,27	0,43
EXT_-X_5G_2kg_X2_Z2cm	1,17	0,94	ISL C4-C5	0,33	0,39	0,28	0,45
EXT_-X_5G_3kg_X-2_Z-2cm	1,24	0,99	ISL C4-C5	0,37	0,40	0,29	0,48
EXT_-X_5G_3kg_X-2_Z6cm	1,22	0,98	ISL C4-C5	0,38	0,49	0,28	0,52
EXT_-X_5G_3kg_X6_Z-2cm	1,21	0,97	ISL C4-C5	0,35	0,40	0,28	0,48
EXT_-X_5G_3kg_X6_Z6cm	1,15	0,92	ISL C4-C5	0,34	0,49	0,26	0,49